**EO-05-002**

# Remedial Investigation Report For the Westinghouse Hematite Site

# Rev 1, Volume 2: Appendices

Prepared for:

Westinghouse Electric Company
Hematite Facility
3300 State Road P
Festus, MO 63028

Prepared by:

Science Applications International Corporation
8421 St. John Industrial Drive
St. Louis, MO 63114
314-770-3000

and

GEO Consultants, LLC
199 Kentucky Avenue
Kevil, KY 42053
270-462-3882

January 2007

**SCIENCE APPLICATIONS INTERNATIONAL CORPORATION**
**AND**
**GEO CONSULTANTS, LLC**

contributed to the preparation of this document and should not be considered an eligible contractor for its review.

**EO-05-002**

# Remedial Investigation Report For the Westinghouse Hematite Site

# Rev 1, Volume 2: Appendices A-L

Prepared for:

Westinghouse Electric Company
Hematite Facility
3300 State Road P
Festus, MO 63028

Prepared by:

Science Applications International Corporation
8421 St. John Industrial Drive
St. Louis, MO 63114
314-770-3000

and

GEO Consultants, LLC
199 Kentucky Avenue
Kevil, KY 42053
270-462-3882

January 2007

**SCIENCE APPLICATIONS INTERNATIONAL CORPORATION**
**AND**
**GEO CONSULTANTS, LLC**

contributed to the preparation of this document and should not be considered an eligible contractor for its review.

# APPENDIX A
# GROUNDWATER MODELING REPORT

**THIS PAGE INTENTIONALLY LEFT BLANK.**

**EO-05-003**

# Groundwater and Contaminant Transport Modeling for the Westinghouse Hematite Site

Prepared for:

Westinghouse Electric Company
Hematite Facility
3300 State Road P
Festus, MO 63028

Prepared by:

Science Applications International Corporation
8421 St. John Industrial Drive
St. Louis, MO 63114
314-770-3000

and

GEO Consultants, LLC
199 Kentucky Avenue
Kevil, KY 42053
270-462-3882

January 2007

**SCIENCE APPLICATIONS INTERNATIONAL CORPORATION**
**AND**
**GEO CONSULTANTS, LLC**

contributed to the preparation of this document and should not be considered an eligible contractor for its review.

**EO-05-003**

# Groundwater and Contaminant Transport Modeling for the Westinghouse Hematite Site

Prepared for:

Westinghouse Electric Company
Hematite Facility
3300 State Road P
Festus, MO 63028

Prepared by:

Science Applications International Corporation
8421 St. John Industrial Drive
St. Louis, MO 63114
314-770-3000

and

GEO Consultants, LLC
199 Kentucky Avenue
Kevil, KY 42053
270-462-3882

January 2007

**THIS PAGE INTENTIONALLY LEFT BLANK.**

# CONTENTS

FIGURES ..... v

TABLES ..... ix

THIS PAGE INTENTIONALLY LEFT BLANK.ACRONYMS ..... x

ACRONYMS ..... xi

1. INTRODUCTION ..... 1

2. SITE HYDROGEOLOGIC CONCEPTUAL MODEL ..... 1

3. POTENTIOMETRIC SURFACES AND GROUNDWATER FLOW DIRECTIONS IN THE HYDROSTRATIGRAPHIC UNITS ..... 2

4. MODFLOW GROUNDWATER FLOW MODELING ..... 3
   - 4.1 MODEL LAYERS ..... 3
   - 4.2 MODEL BOUNDARY CONDITIONS ..... 3
   - 4.3 MODEL CALIBRATION ..... 4

5. MODPATH PARTICLE TRACKING ..... 5

6. REACTIVE TRANSPORT MODELING OF CHLORINATED ORGANICS ..... 6

7. TRANSPORT MODELING OF RADIONUCLIDES ..... 8

8. CONCLUSIONS ..... 9

9. REFERENCES ..... 10

**THIS PAGE INTENTIONALLY LEFT BLANK.**

# FIGURES

Fig. 1. Hematite Facility location shown on topographic map. ..... 15
Fig. 2. Lithologies (a) and hydrostratigraphic units (HSU) (b) underlying the Hematite Site..... 16
Fig. 3. Hydraulic conductivities (ft/day) measured from slug tests in overburden wells. ..... 17
Fig. 4. Well hydrographs from the Jefferson-City Cotter Formation..... 18
Fig. 5. Well hydrographs from the Roubidoux Formation..... 19
Fig. 6. Borehole injection test results (LBG 2002) and hydraulic conductivities from slug testing in bedrock wells (LBG 2002, SAIC 2007). (Plane fitted through points marked "P" was used to define the upper boundary of the Roubidoux HSU layer.)..... 20
Fig. 7. Potentiometric surface (ft above mean sea level) in the deep overburden (coarse-grain) hydrostratigraphic unit, December 2004..... 21
Fig. 8. Potentiometric surface (ft above mean sea level) in the Jefferson City-Cotter hydrostratigraphic unit, December 2004..... 22
Fig. 9. Potentiometric surface (ft above mean sea level) in the Jefferson City-Cotter-Roubidoux contact zone hydrostratigraphic unit, December 2004..... 23
Fig. 10. Potentiometric surface (ft above mean sea level) in the Roubidoux hydrostratigraphic unit, December 2004..... 24
Fig. 11. Plan view of MODFLOW/RT3D model domain for the Hematite Site, bounded by solid black line. [Model grid also shown; blue dots correspond to bedrock well locations; Line A-A' corresponds to the cross-section shown in Fig. 14.)]..... 25
Fig. 12. Plan view of model grid. [The red line corresponds to Joachim Creek; grid cells in Layer 1 that lie along this line are specified head cells; arcs A-D and B-C are specified head arcs in Layers 8 and 9 (see text for more details); Lines S1-S1' and S2-S2' correspond to cross-sections of model grid shown in Figs. 13 and 14, respectively.)]..... 26
Fig. 13. Elevation view of model grids facing southwest. (Refer to Fig. 12 for orientation of cross-section.)..... 27
Fig. 14. Elevation view of model grid, looking northwest (Refer to Fig. 12 for orientation of cross-section.)..... 28
Fig. 15. Hydrostratigraphic units and corresponding layers represented in MODFLOW model. (Cross-section A-A' in Fig. 11, trending northwest-southeast.)..... 29
Fig. 16. Constant property zones within Layer 1. (Zone 1 and Zone 4 correspond to bedrock in the highlands on either side of Joachim Creek Valley; Zone 2 corresponds to the thick, fine-grained sediments in the terrace deposits; Zone 3 corresponds to the thinner, fine-grained deposits in the alluvial sediments.)..... 30
Fig. 17. Constant property zones within Layer 2. (Zone 1 and Zone 4 correspond to bedrock in the highlands on either side of Joachim Creek Valley; Zone 2 corresponds to the thicker, fine-grained sediments in the terrace deposits; Zone 3 corresponds to the thinner, fine-grained deposits in the alluvial sediments.; refer to the text for a description of Zones 2a, 2b and 2c.)..... 31
Fig. 18. Recharge zones for the Hematite Site MODFLOW mode. ..... 32
Fig. 19. Potentiometric surface (ft above mean sea level) in Layer 2 of calibrated steady-state MODFLOW model. (Layer 2 corresponds to the deep overburden HSU.)..... 33
Fig. 20. Potentiometric surface (ft above mean sea level) in Layer 5 of calibrated steady-state MODFLOW model. (Layer 5 corresponds to the Jefferson-City Cotter HSU.)..... 34
Fig. 21. Potentiometric surface (ft above mean sea level) in Layer 8 of calibrated steady-state MODFLOW model. (Layer 8 corresponds to the Jefferson-City Cotter/Roubidoux contact zone HSU.)..... 35

Fig. 22. Potentiometric surface (ft above mean sea level) in Layer 9 of calibrated steady-state MODFLOW model. (Layer 9 corresponds to the Jefferson-City Cotter/Roubidoux contact zone HSU.) ..... 36
Fig. 23. Comparison between modeled and average measured water levels in wells at the Hematite Site. (Deep overburden (OB), Jefferson City-Cotter (JC), and Roubidoux (RB) wells; see the text for a residual summary.) ..... 37
Fig. 24. MODPATH-simulated (forward and backward) particle pathways and travel times. [Blue lines are potentiometric contour lines for layer corresponding to transmissive Jefferson City-Cotter HSU; pumping in private wells at household rates (35 $ft^3$/day).]. *Note that particle pathways indicate groundwater flowlines and are not necessarily contaminant pathways.* ..... 38
Fig. 25. MODPATH-simulated (forward and backward) particle pathways and travel times. [Blue lines are potentiometric contour lines for layer corresponding to Jefferson City-Cotter HSU; specified extraction flow rate in private wells at 2000 $ft^3$/day (~10.4 gpm) drawn from Jefferson City-Cotter HSU layer to simulate vertical borehole flow.) *Note that particle pathways indicate groundwater flowlines and are not necessarily contaminant pathways.* ..... 39
Fig. 26. Simulated PCE concentration contours (mg/L) in layer corresponding to terrace/alluvial deposits at t = 3000 days (~8 years). (Constant concentration source of 200 mg/L PCE placed in cell corresponding to BD-02; simulated using MODFLOW model with vertical borehole flow and RT3D Sequential Decay chemical reaction package.) ..... 40
Fig. 27. Simulated PCE concentration contours (mg/L) in layer corresponding to terrace/alluvial deposits at t = 9000 days (~25 years). (Constant concentration source of 200 mg/L PCE placed in cell corresponding to BD-02; simulated using MODFLOW model with vertical borehole flow and RT3D Sequential Decay chemical reaction package.) ..... 41
Fig. 28. Simulated PCE concentration contours (mg/L) in layer corresponding to terrace/alluvial deposits at t = 15,000 days (~41 years). [Constant concentration source of 200 mg/L PCE placed in cell corresponding to BD-02; simulated using MODFLOW model with vertical borehole flow and RT3D Sequential Decay chemical reaction package; note that there is not much difference when compared to t = 9000 days (Fig. 28); suggests steady-state conditions in contaminant distribution.] ..... 42
Fig. 29. Simulated PCE concentration contours (mg/L) in layer corresponding to transmissive Jefferson City-Cotter Formation at t = 15,000 days (~41 years). [Constant concentration source of 100 mg/L PCE placed in Burial Pits (red square); simulated using MODFLOW model with vertical borehole flow and RT3D sequential decay chemical reaction package (PCE > TCE > *cis*-1,2-DCE > vinyl chloride > ethene); inset graph shows PCE and TCE concentrations versus time at location corresponding to BR-04-JC.] ..... 43
Fig. 30. Simulated TCE concentration contours (mg/L) in layer corresponding to transmissive Jefferson City-Cotter Formation at t = 15,000 days (~41 years). [Constant concentration source of 50 mg/L PCE and 50 mg/L TCE placed in vicinity of Burial Pits (red square); simulated using MODFLOW model with vertical borehole flow and RT3D sequential decay chemical reaction package (PCE > TCE > *cis*-1,2-DCE > vinyl chloride > ethene); note that TCE shown in figure is from degradation of PCE in source.] ..... 44
Fig. 31. Simulated uranium concentration contours (mg/L) in layer corresponding to deep overburden at t = 74,000 days (~200 years). [Constant concentration source of 0.2 mg/L uranium placed in Burial Pits and Deul's Mountain (red squares); simulated using MODFLOW model with vertical borehole flow and RT3D Tracer Transport package (includes partition coefficient measured in site-specific study (SAIC 2003).] ..... 45
Fig. 32. Uranium versus time at grid cell in Layer 4 (Jefferson City-Cotter HSU) near Deul's Mountain Source. (See "resident farmer" location in Fig. 31.) ..... 46

Fig. 33. Uranium versus time at grid cell in Layer 4 (Jefferson City-Cotter HSU) near Burial Pits source. (See “resident farmer” location in Fig. 31.)..... 47

**THIS PAGE INTENTIONALLY LEFT BLANK.**

# TABLES

Table 1. Correspondence between hydrostratigraphic units and layers in the MODFLOW Model, including hydraulic conductivities assigned to layers and zones ..... 51

**THIS PAGE INTENTIONALLY LEFT BLANK.**

# ACRONYMS

| | |
|---|---|
| CSM | conceptual site model |
| DCE | dichloroethylene |
| gpd | gallons per day |
| gpm | gallons per minute |
| HSU | hydrostratigraphic unit |
| PCE | perchloroethylene |
| RI | remedial investigation |
| $^{99}$Tc | technetium-99 |
| TCE | trichloroethylene |
| USGS | U. S. Geological Survey |
| WEC | Westinghouse Electric Company |

**THIS PAGE INTENTIONALLY LEFT BLANK.**

# 1. INTRODUCTION

The Westinghouse Hematite Facility is located near the town of Hematite, in Jefferson County, Missouri. The Hematite Facility became operational in July 1956, producing uranium metals for the nuclear fuel program of the U. S. Navy. In April 2000, Westinghouse Electric Company (WEC) acquired the property when it purchased the nuclear operations of Asea Brown Boveri. WEC ceased operations in June 2001 and is performing site investigation activities in preparation for site remediation, including decommissioning.

The groundwater flow and contaminant transport modeling described in this report is part of the remedial investigation (RI) for the Hematite Site (SAIC 2007). The overall goals of the RI were to characterize the nature and extent of contamination resulting from previous operations at the Hematite Facility, to reasonably predict contaminant fate and transport in the surface and subsurface environment, and to provide sufficient data to facilitate the development of alternatives in a feasibility study for site remediation. The methods and results of the RI field sampling and analyses, which were conducted from April 2004 through January 2005, are described in the *Remedial Investigation Report for the Westinghouse Hematite Site, Rev 1* (SAIC 2007). The RI data were integrated with historical information from previous investigations to develop a conceptual hydrogeologic model for the Hematite Site. Using the conceptual site model (CSM) as a framework, a steady-state finite-difference numerical model was developed and calibrated against water levels from the Hematite Site's monitoring well network. The model was then used to explore contaminant migration pathways from known and suspected sources areas, and to identify flow and transport mechanisms that influenced the current distribution of contamination in the groundwater, as revealed by the sampling and analyses conducted as part of the RI.

As used throughout this document, the "Hematite Facility" (Fig. 1) refers to the central portion of the property, encompassing the historic primary operations area, Site Pond and burial pits areas, while the "Hematite Site" refers to the "Hematite Facility," and other areas which were the focus of this investigation based on potential impacts by previous facility operations.

# 2. SITE HYDROGEOLOGIC CONCEPTUAL MODEL

The Hematite Facility is built upon 20 to 35 ft of terrace/alluvial floodplain sediments overlying bedrock within the valley carved by Joachim Creek (Fig. 2a). Surface elevation within the Hematite Facility ranges from ~420 to ~440 ft. The terrace/alluvium deposits consist primarily of upper fine-grained silts and clay that overlie coarser-grained material (sands-gravels) near the bedrock surface. The thickness of the coarse-grain unit is highly variable in this region, but logs from overburden boreholes (SAIC 2007) show that the sand-gravel layer is relatively thin directly under the Facility (<1 to 2 ft), and thickens toward Joachim creek (5 to 20 ft) as the overburden transitions from terrace deposits near the Hematite Facility to alluvial sediments near Joachim Creek. The varying nature of the sediments is reflected by hydraulic conductivities measured during slug tests in overburden wells, which increase toward Joachim Creek (Fig. 3).

The underlying bedrock formations in the area are the Jefferson City-Cotter and the Roubidoux Formations (Fig. 2a). Regionally, the Jefferson City-Cotter Formation consists predominantly of dolostone with small quantities of shale, chert, and sandstone, while the Roubidoux Formation is a loosely to well-cemented sandstone or a sandy to cherty dolostone containing several distinct sandstone

bodies (Imes and Emmett 1994). Locally, the Roubidoux was more dolomitic and somewhat difficult to visually distinguish from the Jefferson City-Cotter Formation in the field. Thus, during bedrock coring and well installation conducted as part of the RI, a sandstone layer was used as a marker bed for finding the contact zone between the Jefferson City-Cotter and Roubidoux Formations (SAIC 2007). This sandstone layer was observed in all the deeper (> ~100 ft) bedrock boreholes, with the exception of BR-04, which was drilled in an earlier study (LBG 2002).

With respect to the hydrogeology at the Hematite Site, the shallow overburden and deep overburden hydrostratigraphic units (HSUs) generally corresponded with the lithologies observed from the cores (Fig. 2b). In the bedrock, three HSUs (Fig. 2b) were identified based on an integration of borehole injection and slug tests with available bedrock well hydrographs (water level versus time data). The following is a brief summary of how the bedrock HSUs were identified; a more detailed discussion can be found in (SAIC 2007). Figures 4 and 5 show hydrographs from wells screened in the Jefferson City-Cotter Formation, and from wells screened in the Roubidoux Formation. These graphs show that water levels in the Roubidoux wells have risen dramatically (up to 50 ft) since January 2004, but water levels in the Jefferson City-Cotter have virtually been unaffected by the rebound in the Roubidoux Formation. The rebound in the Roubidoux wells was traced to the shut down of water supply production wells in the city of Festus in August 2003 when a water supply system that obtained water from shallow (~100 ft) alluvial sediments of the Mississippi River floodplain was put on line (SAIC 2007). Locally, the connection of residences across Joachim Creek to the public water supply system, in response to contamination found in their wells, and concomitant abandonment of the domestic wells in the residential areas near the Hematite Facility may have also had an impact. The comparison of well hydrographs in Figs. 4 and 5 suggests that there is minimal hydraulic connectivity between the Jefferson City-Cotter and the Roubidoux Formations. This is consistent with observations made in borehole injection tests (see Section 3.4 and borehole logs in LBG 2002) and hydraulic conductivity measurements through slug testing in the bedrock wells (Section 4.7 and Appendix J in LBG 2002, SAIC 2007). The injections tests (Fig. 6) show distinct intervals of high transmissivity separated by a zone of lower transmissivity. A plot of slug test results versus elevation in Fig. 6 also suggests the existence of a depth interval where hydraulic conductivities are relatively low. Integration of the hydraulic conductivity tests with geologic cross-sections indicates that this low transmissivity zone roughly corresponds to the contact zone between the Jefferson City-Cotter and Roubidoux Formations (SAIC 2007). Thus, the CSM for the bedrock at the Hematite Site consists of three HSUs (Fig. 2b): (1) the Jefferson City-Cotter, (2) the Jefferson City-Cotter-Roubidoux contact zone, and (3) the Roubidoux HSU.

# 3. POTENTIOMETRIC SURFACES AND GROUNDWATER FLOW DIRECTIONS IN THE HYDROSTRATIGRAPHIC UNITS

Potentiometric surfaces in the deep overburden and bedrock HSUs are shown in Figs. 7 through 10. These maps are based on a set of water level measurements made in December 2004 as part of the RI (SAIC 2007). In the deep overburden (Fig. 7), groundwater flow is chiefly in a southeastward direction from the Hematite Facility toward Joachim Creek where it discharges. Furthermore, a groundwater mound is associated with the Hematite Facility and has a significant impact on the potentiometric surfaces. Groundwater flow in the Jefferson City-Cotter HSU appears to be affected by this mounding, and components of flow radiate from the Hematite Facility toward the northeast and the southeast within this HSU (Fig. 8). The flow along the northeast is consistent with the orientation of bedding planes that slope in the same direction. The flow towards the southeast may be part of topographically controlled flow from the highlands to the valleys, a pattern that is typical of shallow groundwater in the region (Imes and Emmet 1994). In the Jefferson City-Cotter/Roubidoux contact zone and Roubidoux HSUs (Figs. 9

and 10) the current direction of groundwater flow appears to reflect a northeasterly trajectory, which is consistent with regional groundwater flow direction in the Roubidoux Formation.

# 4. MODFLOW GROUNDWATER FLOW MODELING

A steady-state groundwater MODFLOW (Harbaugh et al. 2000) model was developed based on the CSM described in Chap. 2, and calibrated against average water levels from selected wells. Use of MODFLOW for groundwater modeling implicitly assumes the bedrock formations are suitably modeled as porous media. This is a reasonable approach given that this is the first modeling effort for the Hematite Site, and more complex fracture models should only be pursued if the porous medium model is unable to reproduce the hydrogeologic observations at the Hematite Site.

Flowpath simulations through particle tracking were performed using MODPATH (Pollock 1994), and reactive contaminant transport modeling was conducted using RT3D (Clement 1997, 2003). A finite-difference numerical grid was built using GMS 5.0 (Environmental Monitoring Systems Incorporated, South Jordan, UT), a software tool that serves as a graphical user interface for running MODFLOW, MODPATH, and RT3D simulations.

## 4.1 MODEL LAYERS

Figure 11 shows the MODFLOW model domain, which encompasses a larger region than the Hematite Site, so that assumptions at the model boundaries would not significantly impact flow simulations within the area of interest. The grid cell dimensions were adjusted so that grid cells were smaller in the vicinity of the Hematite Site (Figs. 11 and 12). The model grid consists of nine layers (Figs. 13 and 14), with layers generally corresponding to the HSUs as shown in Fig. 15. The top surface of Layer 1 (see elevation views of grid in Figs. 13 and 14) was modeled using a 30-min digital elevation model obtained from the U. S. Geological Survey (USGS). The bottoms of Layers 1 through 5 were specified by subtracting fixed-increment distances from the top of Layer 1, creating layers with constant thickness that follow topography. The top of Layer 9 (representing the Roubidoux Formation) was made to conform to the lower transmissive zone indicated by the borehole injection tests by fitting a plane through the points at each borehole above the high injection rates (see points marked with “P” in Fig. 6). The resulting plane has a strike of 17° northwest and a dip of 2° northeast, roughly conforming to the regional strike and dip of the bedrock formations. Layers 1 and 2 were further subdivided into zones, so that different hydraulic conductivities can be assigned to different zones that correspond to the terrace and alluvial deposits (Figs. 16 and 17). Also, within Layer 2, several zones were defined around the footprint of the Hematite Facility in anticipation of needing to simulate groundwater mounding by varying hydraulic conductivities.

## 4.2 MODEL BOUNDARY CONDITIONS

Cells within the top model layer that coincided with Joachim Creek (Fig. 13) were “specified head” cells. Attempts were made to specify heads at cells in the model that corresponded to the Lake Virginia tributary, Site Creek, and Northeast Site Creek. However, specifying heads to represent these streams was exerting an influence on the simulated hydraulic heads that was not observed in the monitoring well data. The “river” boundary condition was then used, where the interaction of streams and groundwater is simulated through a streambed with a specified conductance. The streambed conductance had to be set to very low values to match measured water levels. As a result, the influence of these surface streams on the

groundwater was ignored in the final calibrated model. The latter assumption is consistent with the fine-grained nature of the shallow soils at the Hematite Site, which probably limit leakage from the surficial (some intermittent) streams to groundwater. With the exception of the bottom two layers of the model, the boundaries of all the other layers (solid line in Fig. 11) were specified as no-flow boundaries. For the bottom two layers of the model, heads were specified along arc A-D and arc B-C in Fig. 12, resulting in a regional northeasterly direction in the deeper layers of the model. This is consistent with the regional flow direction inferred from the water level data from the Roubidoux wells in December 2004 (Fig. 10).

Figure 18 shows the zones of constant recharge applied to the top of the model. As described later, the recharge rate in a small zone within the Burial Pit Area (Zone 1 in Fig. 1) had to be set to a high value to simulate mounding underneath the Hematite Facility.

## 4.3 MODEL CALIBRATION

The model was calibrated using the average of historical water levels from deep overburden wells and water level data from April through December 2004 from the bedrock wells. Although water level data were collected from the Roubidoux wells before April 2004, only the data after the significant water level rebound observed in 2003 and 2004 (Fig. 5) were included when calculating the average water level for model calibration. Initial attempts at model calibration also included historical data from the pre-RI shallow overburden wells (screened within the fine-grained layer of the overburden). These initial attempts to simulate the water levels in the shallow overburden wells resulted in unreasonable recharge and high heads in the underlying layers. This might have been due to the perched nature of the groundwater in the shallow overburden (SAIC 2007), trapped over a low-conductivity soil (the “fat clay” as identified by LBG 2002), which was not explicitly represented in the layer model. Incorporating this low-conductivity unit into the model would have required multiple layers to represent the shallow overburden, which would have increased the number of model grid cells and numerical resources to solve the larger set of equations. Since flow in the shallow overburden is predominantly downward (SAIC 2007), and off-site contaminant transport is likely from lateral flow through the deep overburden and bedrock, calibration to the shallow overburden wells was discontinued and only the deep overburden and bedrock wells were considered in the final calibrated model.

Initial estimates for hydraulic conductivities of the layers were based on historical and RI slug test results (Figs. 3 and 6), but were later adjusted during model calibration. Table 1 shows the hydraulic conductivities in the final calibrated model generally conform to the relative transmissivity of the various formations observed during the slug tests (SAIC 2007). The hydraulic conductivity in the shallow overburden next to Joachim Creek was set to a high value to correspond to the much thicker coarse-grained and highly conductive alluvial sediments in this area (see Fig. 3). Attempts were made to vary the hydraulic conductivities of Zones 2a through 2c to simulate mounding at the Hematite Site, but, ultimately, this was reproduced by using a high recharge in the Burial Pit area (see below). The hydraulic conductivity of the top layer (Layer 3) had to be set to a low value; otherwise, levels in the overlying deep overburden HSU (Layer 2) were too low. The hydraulic conductivity of Layers 4 and 5 corresponding to the Jefferson City-Cotter HSU was set to 5 ft/day, with an anisotropy factor of 5 (to simulate the effects of bedding fractures). Slug testing in the Jefferson City-Cotter HSU indicated higher conductivities in some of the wells. However, the slug test measurements were also highly variable, spanning two orders of magnitude so that the average hydraulic conductivity of the slug tests in the Jefferson City-Cotter wells (geometric average was 2.6 ft/day) was much lower than the highest value measured value (104 ft/day). The hydraulic conductivity for Layers 6 through 8, representing the Jefferson City-Cotter contact zone HSU, was set to 0.002 ft/day. This value was arrived at through successive simulations where the conductivity for this layer was lowered until changes in hydraulic heads within Layer 9 (representing the

Roubidoux HSU) did not affect hydraulic heads in Layers 4 and 5 (representing the Jefferson City-Cotter HSU). This is consistent with the lack of hydraulic interconnectivity between the Jefferson City-Cotter and Roubidoux HSUs inferred from time series water level data and hydraulic conductivity tests, as described in Chap. 2. The hydraulic conductivity assigned to Layers 6 to 8 (0.002 ft/day or 7 × 10-7 cm/s) is within the range of hydraulic conductivities reported for limestone and dolomite (Freeze and Cherry 1979).

To capture mounding under PZ-04 (see Fig. 8), a high recharge had to be assigned to the northern area of the Burial Pits (0.05 ft/day in Zone 1, compared to 0.0002 ft/day in Zones 2 and 3, and 0.0005 ft/day for Zones 4 through 8 in Fig. 18). A higher recharge value over the Burial Pits is plausible because buried objects and the use of limestone gravel as fill for the Burial Pits (SAIC 2007) would have resulted in a more permeable layer that is more conductive to percolation of rainfall water to the subsurface. Note however, that 0.05 ft/day is about five times the precipitation rate in the area (~40 in./year or 0.01 ft/day), suggesting other sources of water other than direct percolation of rainwater. Furthermore, this high recharge alone could not simulate the high heads in the PZ-04 area. To simulate these heads, an "injection well" flowing at a rate of 2000 $ft^3$/day (~10.4 gpm) was added as a source in the northeastern end of the plant. This "injection well" possibly represents leakage from water distribution pipelines or drainage systems, shallow overland flow from the highlands north of the Facility, or run-off from the highway. With the combined high recharge in the Burial Pits and the injection well, the mounding under PZ-04 was reproduced (see MODFLOW-generated potentiometric maps in Figs. 19 through 22).

A comparison between the modeled and calibrated hydraulic heads is shown in Fig. 23, where a perfect match is represented by the 1:1 line. Following ASTM D 5490-93 (ASTM 1993), the average residual for the final calibrated model is -0.6 ft, with average residuals of -0.02, -1.8, and 0.6 in the deep overburden, Jefferson City-Cotter, and Roubidoux wells, respectively. These residuals are acceptable because they are comparable to the seasonal water level fluctuations observed in the wells.

# 5. MODPATH PARTICLE TRACKING

MODPATH and the calibrated steady-state flow model were used to gain insight into possible sources of chlorinated solvent contamination detected in bedrock wells BR-08-JC, BR-09-JC, and BR-04-JC (see Fig. 20 for well locations; also in SAIC 2007). Using the "backward" tracking capability, MODPATH simulations indicate that particles at these locations all have their "sources" in the vicinity of the Burial Pit Area (Fig. 24). Forward particle tracking indicated that particles at these locations will be advected towards Joachim Creek. Particle path lines and travel times (Fig. 24) vary significantly depending on the "release point" of the particles within the Hematite Facility. Path lines originating from "source zones" towards the southwestern part of the Hematite Facility (e.g., BD-02) are directed toward the southeast following the hydraulic gradient toward Joachim Creek. Travel times for these particles are three times higher than for some particles that are "released" within the Burial Pit area (i.e., ~30 versus ~10 years, respectively, see Fig. 24). An elevation view of the path lines (not shown) reveals that the particles from the Burial Pit area move down and travel toward Joachim Creek mostly within the Jefferson City-Cotter HSU, resulting in shorter travel times than particles from BD-02, which stay mostly within the layer representing the alluvial/terrace deposits. The hydraulic conductivity for this layer is high near Joachim Creek (e.g., Zone 3, Fig. 17), but is an order of magnitude lower near the Hematite Facility (e.g., Zone 2, Fig. 17). The path lines in Fig. 24 show a radial pattern from the Burial Pit area, influenced by mounding of groundwater in the vicinity of PZ-04. The model predicts that path lines directed toward BR-04 turn toward Joachim Creek as the influence of the mound diminishes. Note that the boundary conditions for the groundwater model implicitly constrain most of the groundwater within the shallow bedrock (e.g., Jefferson City-Cotter HSU represented by Layers 3 through 5) to discharge into Joachim

Creek, and that the regional northeasterly flow exists in the lower (Layers 8 and 9) layers. However, it is uncertain that groundwater and dissolved contaminants in BR-04-JC (found at a depth of 95 to 105 ft below ground surface, SAIC 2007) actually discharge into Joachim Creek, as shown by model output. It is possible that at this depth the regional northeasterly flow direction is dominant.

The flow model used for particle tracking includes a simulation of domestic well pumping by specifying well extraction flows at all the wells shown in Fig. 24 (labeled "PW"). The domestic well pumping rate was estimated from 2000 USGS water use data (Hutson et al. 2005), which stated that for Jefferson County, Missouri, the total population that used self-supplied water was $51.57 \times 10^3$, and the total groundwater withdrawal from domestic wells was $3.35 \times 10^6$ gpd, from which the estimated per capita water usage is 65 gpd, or 260 gpd (35 $ft^3$/day) for a household with four members. Although this flow rate was applied to all the domestic wells shown in Fig. 24 (labeled "PW"), all the pathlines shown in this figure indicate discharge to Joachim Creek. Thus, the numerical modeling suggests that the impact of pumping in the domestic wells (assumed to be equivalent to a steady extraction rate of 35 $ft^3$/day) was not enough to draw groundwater from the Hematite Facility side of Joachim Creek into the area where the domestic wells are located.

In *Remedial Investigation Report for the Westinghouse Hematite Site, Rev 1* (SAIC 2007), vertical borehole flow was suggested as a possible mechanism behind contaminants moving under Joachim Creek toward the residential wells. Prior to August 2003, there was a large head difference between the Jefferson City-Cotter and Roubidoux Formations (see Figs. 4 and 5). Because open-hole construction was used in the domestic wells, this head difference may have been sufficient to induce inter-aquifer flow with the open boreholes as conduits. When an extraction rate of 2000 $ft^3$/day (10.4 gpm) was applied to 13 wells in the vicinity of PW-19 to simulate vertical borehole flow, a significant impact on the potentiometric surface is observed, as well as on path lines from BR-08 and BR-09 that now go under Joachim Creek into PW-19 and PW-16 (Fig. 25). Note that 10 gpm is the lowest flow rate observed by Metz and Brendle (1996), who measured vertical borehole flow rates in 87 open borehole wells in Florida. Because water levels in the Roubidoux have rebounded (Fig. 3.27 in Chap. 3 of the RI; SAIC 2007) and the driving force for this vertical flow rate is no longer present, it is difficult to estimate the actual flow rates that previously existed in the open borehole domestic wells in the PW-19 area. Nevertheless, the numerical modeling and simulation shown in Fig. 25 support the suggested impact of vertical borehole flow.

# 6. REACTIVE TRANSPORT MODELING OF CHLORINATED ORGANICS

Contaminant transport modeling using RT3D was coupled with the MODFLOW model for the Hematite Site that includes vertical borehole flow (Fig. 25) to simulate the migration of contaminants from known and suspected source zones at the Hematite Facility. Matching measured contaminant concentrations with modeled values was not attempted because of the existence of multiple sources and the uncertainty of when these sources were emplaced (e.g., t = 0 for the simulations). As such, the primary purpose of these simulations is to investigate the influence of flow patterns (e.g., radial flow around PZ-04) and potential attenuation mechanisms (e.g., sorption and degradation) on the migration of contaminants at the Hematite Site. Longitudinal dispersivities in layers representing the overburden and bedrock HSUs were 100 and 300 ft, respectively, with the vertical and horizontal dispersivities set at a fraction (0.2) of the longitudinal dispersivity. Specified porosities in the overburden and bedrock layers were 0.3 and 0.1, respectively. Previous measurements of organic content in overburden soil samples (average of 0.48% in four samples that were mostly finer-grain; SAIC 2003) were coupled with published values of $K_{om}$ (partition coefficient of a chemical on natural organic matter) to arrive at sorption

coefficients for perchloroethylene (PCE) (1.74 L/kg); trichloroethylene (TCE) (0.6 L/kg); *cis*-1,2-dichloroethylene (DCE) (0.23 L/kg); and vinyl chloride (0.04 L/kg). Because natural organic matter is likely to be low in bedrock, zero $K_d$ values (i.e., no sorption) were specified for the bedrock model layers. Degradation was simulated using the Sequential Decay Reaction package of RT3D, which assumed first-order decay kinetics and the following sequence of degradation: PCE > TCE > 1,2-*cis*-DCE > vinyl chloride (Clement 1997). Seven reaction parameters are required for the simulation: four of the parameters are the first-order degradation constants for each of the contaminants in the sequence, and three of the parameters define the yield (e.g., number of moles of TCE produced per mole of PCE). The yield parameters were taken from established stoichiometric equations for sequential degradation of PCE and TCE ($Y_{TCE_PCE}$ = 0.792, $Y_{DCE_TCE}$ = 0.738, and $Y_{VC_DCE}$ = 0.644, Clement 1997). Degradation constants are site-specific because they depend on the nature of the microbes involved in the degradation reactions, as well as the geochemical environment. Although there is clear evidence for reductive dechlorination of PCE and TCE occurring at the site (SAIC 2007), site-specific degradation parameters have not been determined. Thus, degradation constants comparable to literature values (e.g., Newell et al. 1992) were used for the modeling described below. This was deemed to be a reasonable approach since the primary purpose of the modeling is to explore the general impact of flow patterns and attenuation mechanisms rather than to match simulation results with measured groundwater concentrations.

Figures 26 through 28 show simulated PCE concentration contours in the layer corresponding to the deep overburden HSU (Layer 2). The contours emanate from a constant concentration source of 200 mg/L of PCE located at overburden well BD-02, which is located within one of the Hematite Facility's buildings (Building 253). A PCE concentration of 200 mg/L was measured in a groundwater sample from this well collected in December 2004 as part of the RI (SAIC 2007). Co-located soil samples also showed levels of PCE that indicated the presence of a pure (undissolved) phase. Thus, there appears to be source of PCE in the vicinity of BD-02. Degradation constants were as follows: 0.001/day for PCE, TCE, and VC and 0.0004/day for *cis*-1,2-DCE (reflecting the apparent "stalling" of the degradation process at *cis*-1,2-DCE; SAIC 2007). Figures 26 through 28 present model results for t = 3,000 days (~8 years); 9,000 days (~25 years); and 15,000 days (~41 years). Two observations can be made from Figs. 26 through 28: (1) sorption and degradation result in a significant attenuation in PCE levels such that concentrations rapidly drop by one or two orders of magnitude just a short distance from the source (i.e., BD-02), and (2) minimal change between the contour plots at t = 25 years and t = 41 years suggests that a steady-state configuration of the plume is possible if degradation occurs. The predicted plume also tends to be narrow and is directed toward Joachim Creek.

Figure 29 shows another simulation, using the same sorption parameters used in Figs. 26 through 28 but with a 100-mg/L PCE source placed in the northern part of the Burial Pits (see red square in Fig. 29). The degradation parameters were reduced by an order of magnitude to determine whether even at lower degradation rates (all set to 0.0001/day) steady-state conditions can be attained within approximately the same time frame as in the previous simulation. Figure 29 shows simulated PCE concentrations in Layer 5 (corresponding to the Jefferson City-Cotter HSU) at t = 15,000 (~41 years). The predicted PCE plume is approaching a near-steady-state at t = 15,000 days, as shown by a plot of simulated PCE and TCE concentrations versus time at the location corresponding to BR-04-JC (see insert in Fig. 29). The simulation also indicates an elongate PCE plume configuration that is directed towards BR-04, but also encompasses WS-30, WS-31, BR-09, and BR-08. Spreading along the lateral axis of the plume may partially be from the radial flow that is induced by groundwater mounding under the Hematite Site. Lateral spreading is also controlled by the horizontal dispersivity, which was set at 1/5th of the longitudinal dispersivity in the simulation. Figure 30 shows still another simulation where the source is located in the southern part of the Burial Pit area and consists of specified PCE and TCE concentrations of 50 mg/L. The same degradation and sorption parameters are used as in the simulation in Fig. 29, but the overall shape of the PCE and TCE plume in Fig. 29 is elongated toward the southeast in the direction of Joachim Creek. As in particle tracking simulations (Chap. 5), this suggests that contaminant pathways

vary depending on the location of the source, even in the relatively small area of the Burial Pits. This is another illustration of how mounding under the Hematite Site near the Burial Pits may have an impact on contaminant migration away from sources within the Hematite Facility. Figure 29 also illustrates the movement of TCE toward the PW-19 area under the influence of vertical borehole flow in the open boreholes. Note that the model shows contamination spreading to BR-07, which is not consistent with the packer testing and sampling from this well location, which showed minimal to no contamination (SAIC 2007). The transmissivity of the formation around BR-07 may be lower than PW-19, thus reflecting smaller-scale heterogeneities that cannot be captured in the model. Another explanation is related to the details of how the contaminant plume in the Jefferson City-Cotter HSU responded to the various open-hole wells in which vertical borehole flow was occurring. The approaching plume would tend to split apart with different segments migrating preferentially to those wells having more vertical borehole flow. In this way, it is possible that BR-07 may be located in a region bypassed by the different plume segments and not be subject to the influx of significant contamination.

The transport simulations indicate vertical spreading of the contamination (results not shown) in the bedrock even though the vertical dispersivity was only set to 1/5th of the longitudinal dispersivity. This is in contrast to the relatively narrow (20 to 30 ft) zones of contamination observed during packer testing of the newly drilled boreholes (SAIC 2007). This discrepancy may be due to use of a porous medium model to simulate a situation where transport is through discrete fractures. The porous medium model was useful in exploring hydraulic and contaminant transport mechanisms that would explain the observed distribution of contaminants in the overburden and bedrock. If more accurate resolution of these issues is required, the use of fracture flow and transport modeling should also be considered for future modeling efforts.

# 7. TRANSPORT MODELING OF RADIONUCLIDES

Radionuclide transport modeling was performed with sources of uranium (specified concentration of 0.2 mg/L) in the deep overburden HSU (Layer 2) at Deul's Mountain and the Burial Pits, corresponding to the locations where elevated uranium concentrations were measured in groundwater samples (SAIC 2007). A contour plot of uranium concentrations within the deep overburden HSU layer shows very limited movement of uranium from the sources (Fig. 31). Note that the partition coefficient ($K_d$) measured in the site-specific study (175 mL/g; SAIC 2003) was used for the transport model. The $K_d$ factor for uranium is two orders of magnitude higher than the $K_d$ factor for PCE (1.74 mL/g). Thus, it is not surprising that PCE and other chlorinated organics are much more widespread at the Hematite Site than uranium. Although technetium-99 ($^{99}$Tc) transport was not simulated, similar observations regarding limited mobility are expected since the site-specific $K_d$ factor for $^{99}$Tc (106 mL/g) is comparable to that measured for uranium. The site-specific $K_d$ value for $^{99}$Tc is higher than reported literature values. However, significant adsorption of $^{99}$Tc on Hematite Facility sediments was confirmed by retrieval of sorbed $^{99}$Tc from the sediments during the $K_d$ measurements (SAIC 2003).

Time series plots of uranium in grid cells that are located in Layer 4 (corresponding to the Jefferson City-Cotter HSU) near the Deul's Mountain source and near the Burial Pit source are shown in Figs. 32 and 33, respectively. The locations of these grid cells are shown in Fig. 31 and correspond to breakthrough curves for a "resident-farmer" scenario in RESRAD modeling (Yu et al. 2001). Comparison of Figs. 32 and 33 shows much higher uranium concentrations moving into the bedrock near the Burial Pit source. As in the particle tracking and chlorinated organics transport simulations, the modeling suggests that mounding in the area around PZ-04 causes a larger downward component in flow and radionuclide transport in areas near this groundwater mound.

# 8. CONCLUSIONS

A steady-state groundwater MODFLOW model was developed for the Hematite Site. The model layers and hydraulic conductivities were based on the CSM that was developed from an integration of field data collected from previous studies and the recent RI (SAIC 2007). The model was calibrated against the average of historical water levels from wells in the deep overburden and the Jefferson City-Cotter HSU; only water levels from April through December 2004 in the Roubidoux wells were used in the calibration because prior to this period, these wells were undergoing a significant amount of rebound that was traced to the shut down of production wells in the city of Festus. Using the calibrated groundwater flow model, particle tracking using MODPATH and contaminant transport modeling using RT3D were performed. The transport modeling was aimed at exploring the general impact of flow patterns and attenuation mechanisms (i.e., sorption and degradation) on contaminant distribution, rather than matching modeled with measured concentrations. The primary findings of this modeling effort are:

- The shallow groundwater mound underlying the Hematite Facility plays a major role in flow/transport in both layers of the overburden, as well as in the Jefferson City-Cotter HSU.

- The assignment of reasonable downhole flow rates to the open boreholes in the vicinity of PW-19 is essential for creating the observed transport to the southeast in the Jefferson City-Cotter HSU and is supportive of the CSM developed as part of the RI (SAIC 2007).

- Particle tracking was used to identify potential source zones associated with observed contamination in bedrock wells. Backward particle tracking from contaminated bedrock wells (BR-08-JC, BR-09-JC, and BR-04-JC) suggests the Burial Pits to be the source of contamination in these wells. Particle travel times vary depending on the location of their release points within the Hematite Facility. Particles "released" within the southwestern part of the Hematite Facility (i.e., BD-02) tend to have longer travel times toward their discharge point (Joachim Creek) when compared to particles "released" within the northeastern part of the Hematite Facility (i.e., the Burial Pits). This suggests that migration from sources within the northeastern part of the Hematite Facility may be faster than migration from sources in the southwest part of the Hematite Facility. This is due to the mounding in the northeastern corner of the Hematite Facility that causes downward migration in this area to transmissive bedrock formations that are conductive and probably have lower porosities than the overburden.

- Contaminant transport modeling of PCE and TCE in groundwater indicates that sorption and degradation can significantly attenuate contaminant migration such that organic contaminant levels can decrease by one to two orders of magnitude within close proximity of the source areas. Consistent with the particle tracking results, the configuration of the simulated plumes varied depending on the location of the plume's source.

- Contaminant transport modeling of uranium in groundwater indicates very limited spreading of contamination from source areas, consistent with what was observed in groundwater sample data. The site-specific partition coefficient for uranium is two orders of magnitude higher than the sorption coefficient for organics, resulting in significantly less migration for uranium in groundwater at the Hematite Site when compared to PCE and TCE. Although a technetium transport simulation was not performed, limited mobility is also expected for this radionuclide because the site-specific partition coefficient measured during a previous study was comparable to that for uranium. Simulated breakthrough curves for RESRAD "resident farmers" in the immediate vicinity of sources in the Burial Pits and Deul's Mountain were generated from the transport simulations. As in the particle tracking and chlorinated organic transport simulations, the impact of the mound under PZ-04 was apparent from the breakthrough curves that show higher concentrations near the Burial Pits when

compared to Deul's Mountain. The simulation suggests mounding creates a downward flow component that carries contaminants deeper into the bedrock in the areas near the groundwater mound.

# 9. REFERENCES


ASTM (American Society for Testing and Materials) 1993. *Standard Guide for Comparing Ground-Water Flow Model Simulations to Site-Specific Information, ASTM D5490-93* (Reapproved 2002).

Clement, R.T. 1997. *RT3D (Version 1.0) A Modular Computer Code for Simulating Reactive Multispecies Transport in 3-Dimensional Groundwater Systems,* Pacific Northwest National Laboratory, PNNL-11720.

Clement, R.T. 2003. *RT3D Version 2.5 Update Document,* Pacific Northwest National Laboratory.

Pollock, David W. 1994. *User's Guide for MODPATH/MODPATH-PLOT, Version 3: A particle tracking post-processing package for MODFLOW, the U. S. Geological Survey finite-difference ground-water flow model*, U. S. Geological Survey Open-File Report 94-464.

Freeze, R.A. and Cherry, J.A. 1979. *Groundwater,* Prentice-Hall, Englewood Cliffs, NJ.

Harbaugh, A., Banta, E.R., Hill, M.C. and McDonald, M.G. 1992. *MODFLOW-2000, The U. S. Geological Survey Modular Ground-water Model – User Guide to Modularization Concepts and the Ground-Water Flow Process,* U. S. Geological Survey Open-File Report 00-92.

Hutson, Susan S., Barber, N.L., Kenny, J.F. Kristin, Linsey, S., Lumia, D.S., and Maupin, M.A. 2005. *Estimated Use of Water in the United States in 2000,* U. S. Geological Survey Circular 1268, February, http://water.usgs.gov/watuse/data/2000/index.html.

Imes, J.L. and Emmett, L.F. 1994. *Geohydrology of the Ozark Plateaus Aquifer System in Parts of Missouri, Arkansas, Oklahoma, and Kansas,* U. S. Geological Survey Professional Paper 1414-D.

LGB (Leggett, Brashears, & Graham, Inc.) 2002. *Water Wells within Two Mile Radius of the Hematite Site, Jefferson County, Missouri,* Prepared for the Westinghouse Electric Company, May.

Metz, P. and Brendle, D. 1996. *Potential for Water-Quality Degradation of Interconnected Aquifers in West-Central Florida,* U. S. Geological Survey Water-Resources Investigations Report 96-4030.

Newell, C.J., Rifai, H.S., Wilson, J.T., Connor, J.A., Aziz, J.A., and Suarez, M.P. 1992. *Calculation and Use of First-Order Rate Constants for Monitored Natural Attenuation Studies,* Ground Water Issue, U. S. Environmental Protection Agency EPA/540/S-02/500, November.

SAIC (Science Applications International Corporation) 2003. *Determination of Distribution Coefficients for Radionuclides of Concern at the Westinghouse Hematite Facility,* Prepared for Westinghouse Electric Company, December.

SAIC 2007. Remedial Investigation Report for the Westinghouse Hematite Site, Prepared for Westinghouse Electric Company, Prepared by SAIC and GEO Consultants, January.

Yu, C., Cheng, Z.J. LePoire, J.J., Gnanaprajasan, D.J., Kamboj, E., Arnish, S. Wallo III, J. William, and Peterson, H. 2001. *User's Manual for RESRAD Version 6, ANL/EAD-4, Argonne National Laboratory, Argonne, IL*.

**THIS PAGE INTENTIONALLY LEFT BLANK.**

# FIGURES

**THIS PAGE INTENTIONALLY LEFT BLANK.**

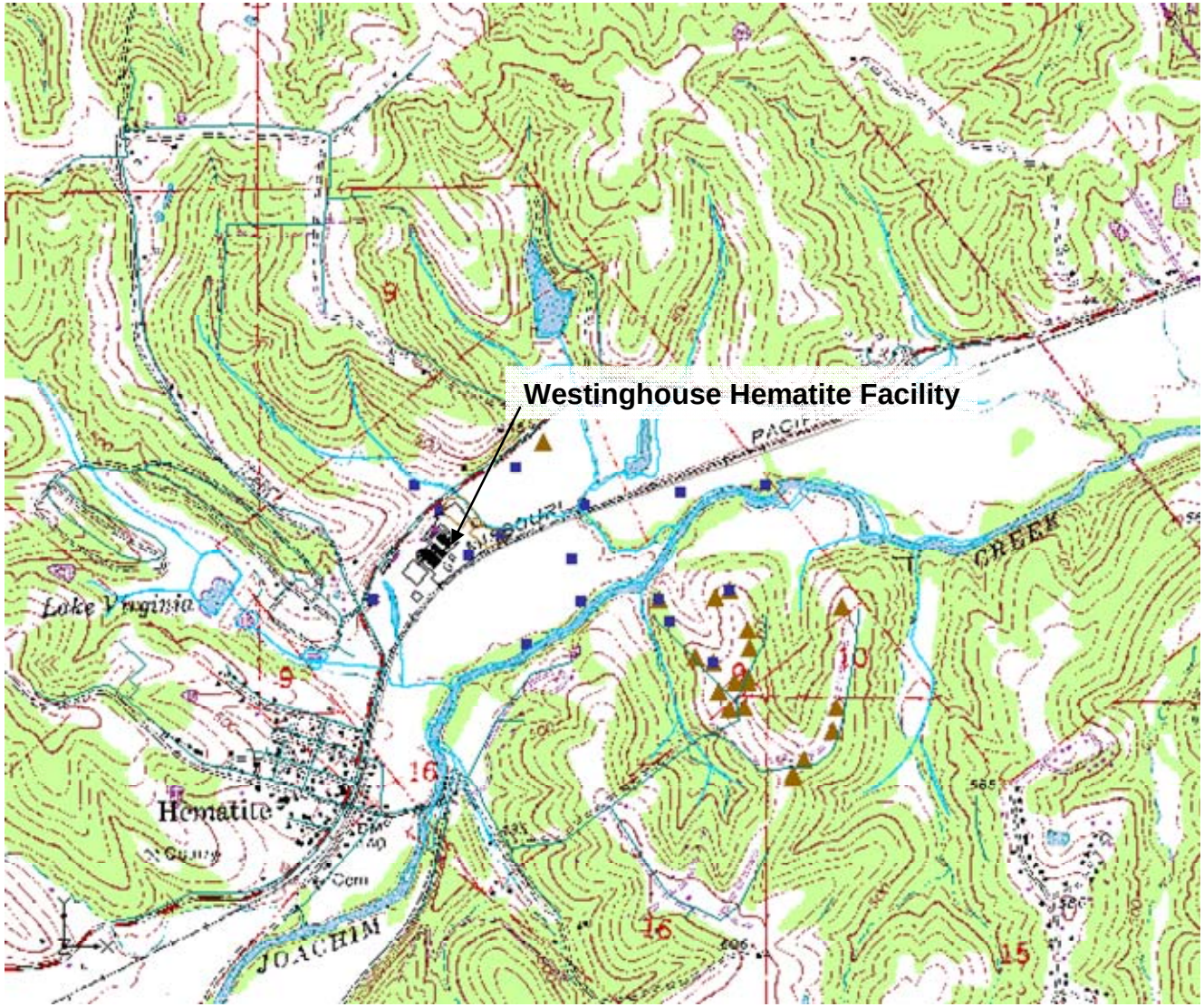


**Fig. 1. Hematite Facility location shown on topographic map.**

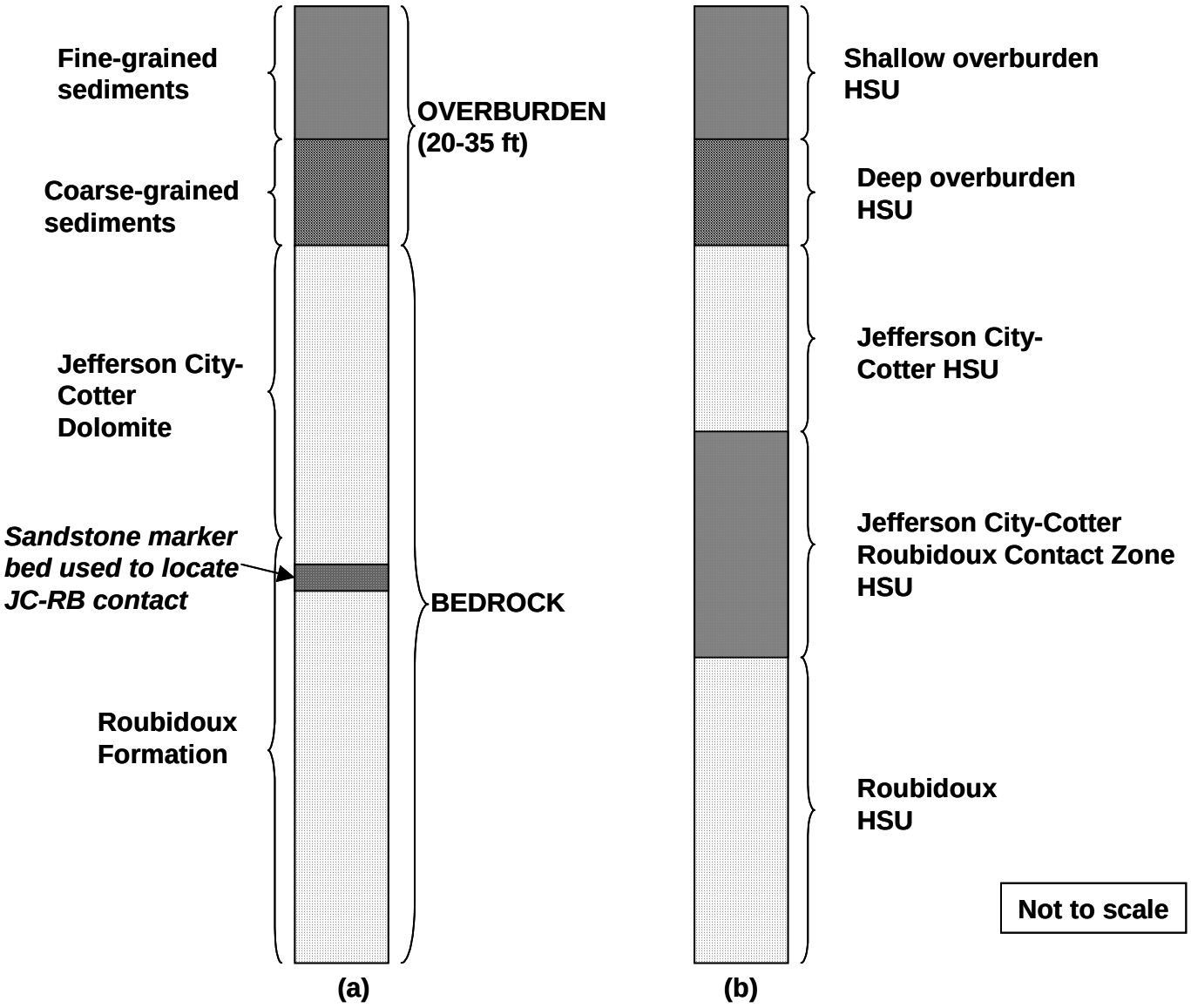


**Fig. 2. Lithologies (a) and hydrostratigraphic units (HSU) (b) underlying the Hematite Site.**

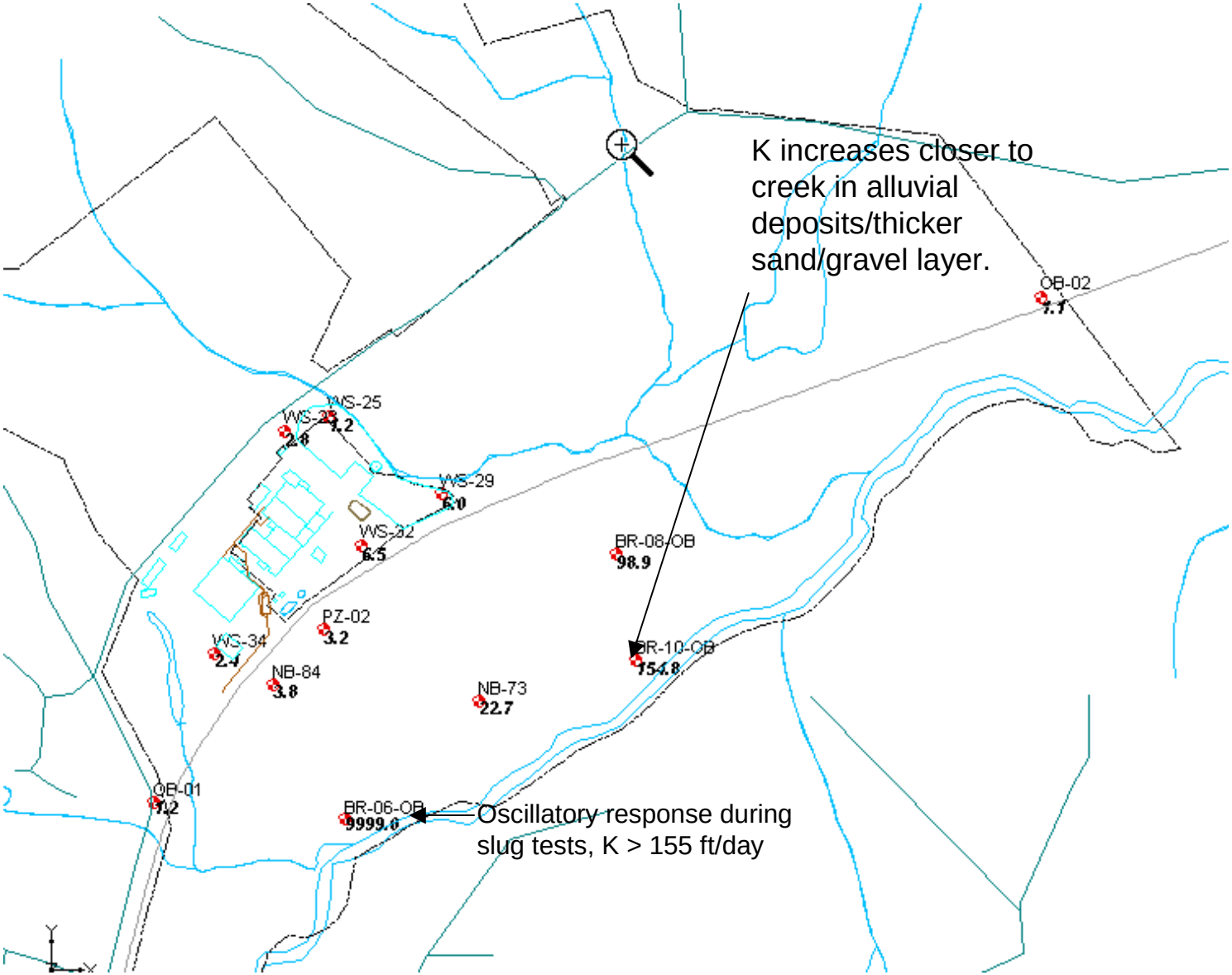


**Fig. 3. Hydraulic conductivities (ft/day) measured from slug tests in overburden wells.**

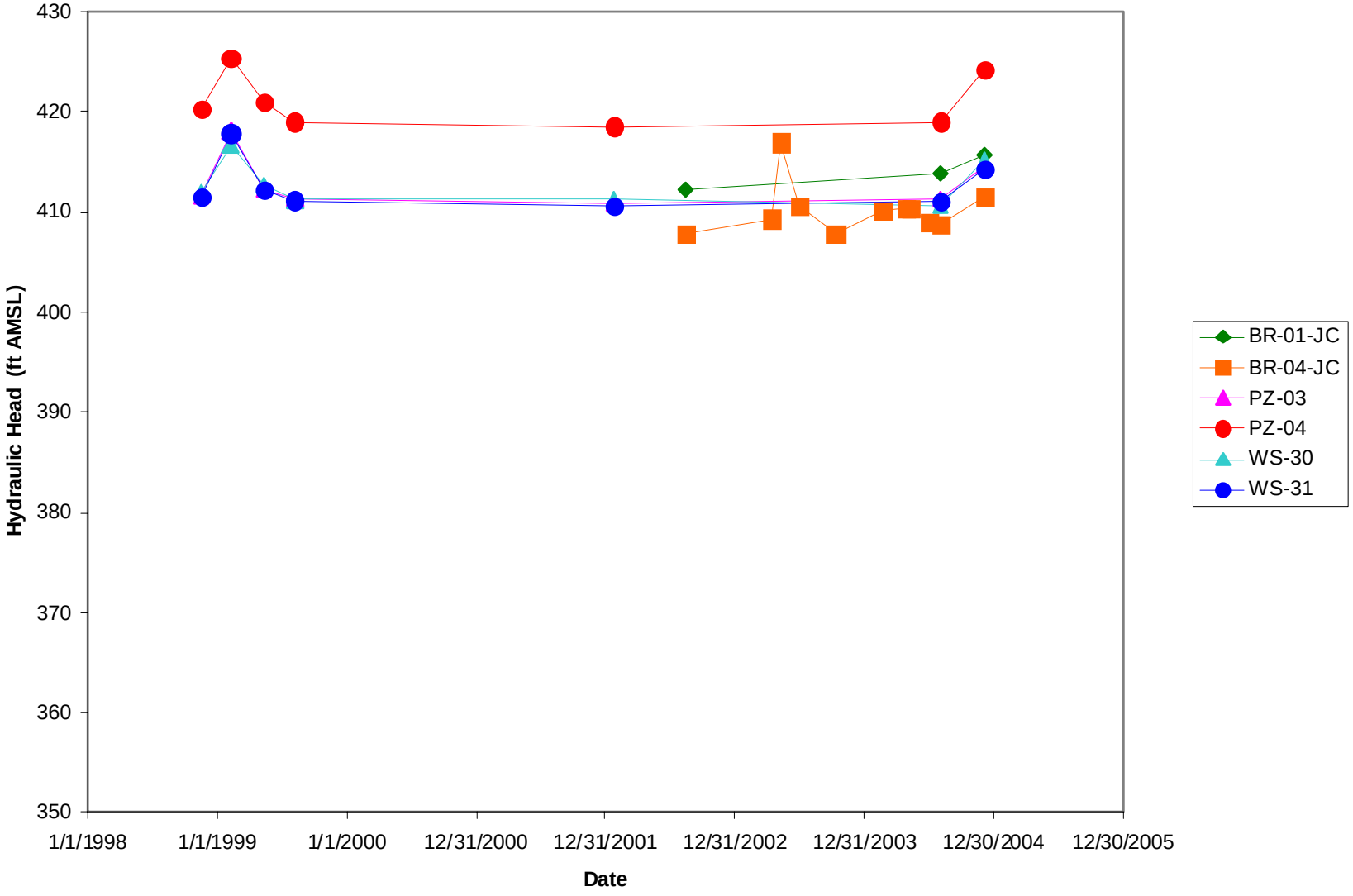


**Fig. 4. Well hydrographs from the Jefferson-City Cotter Formation.**

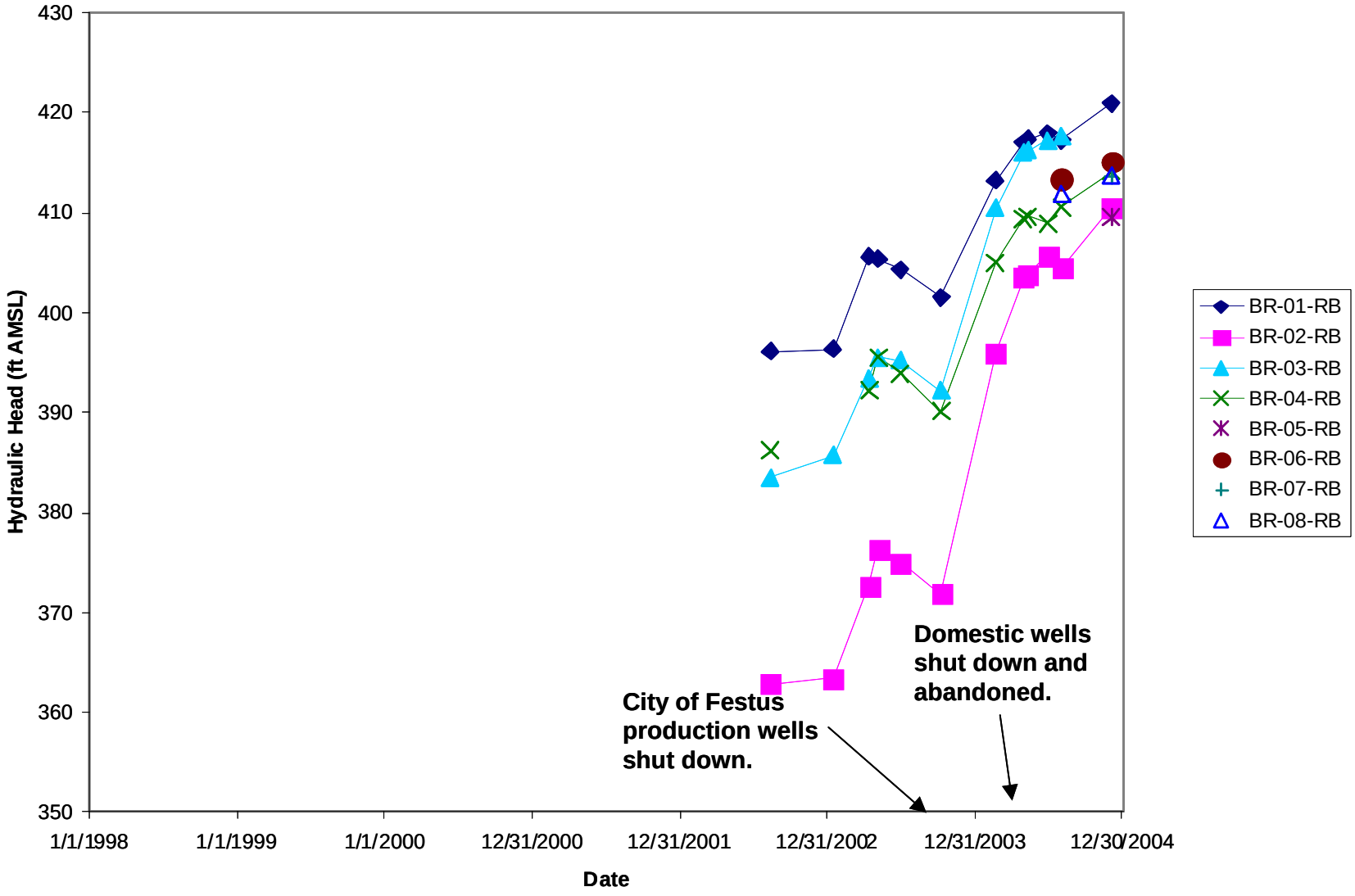


**Fig. 5. Well hydrographs from the Roubidoux Formation.**

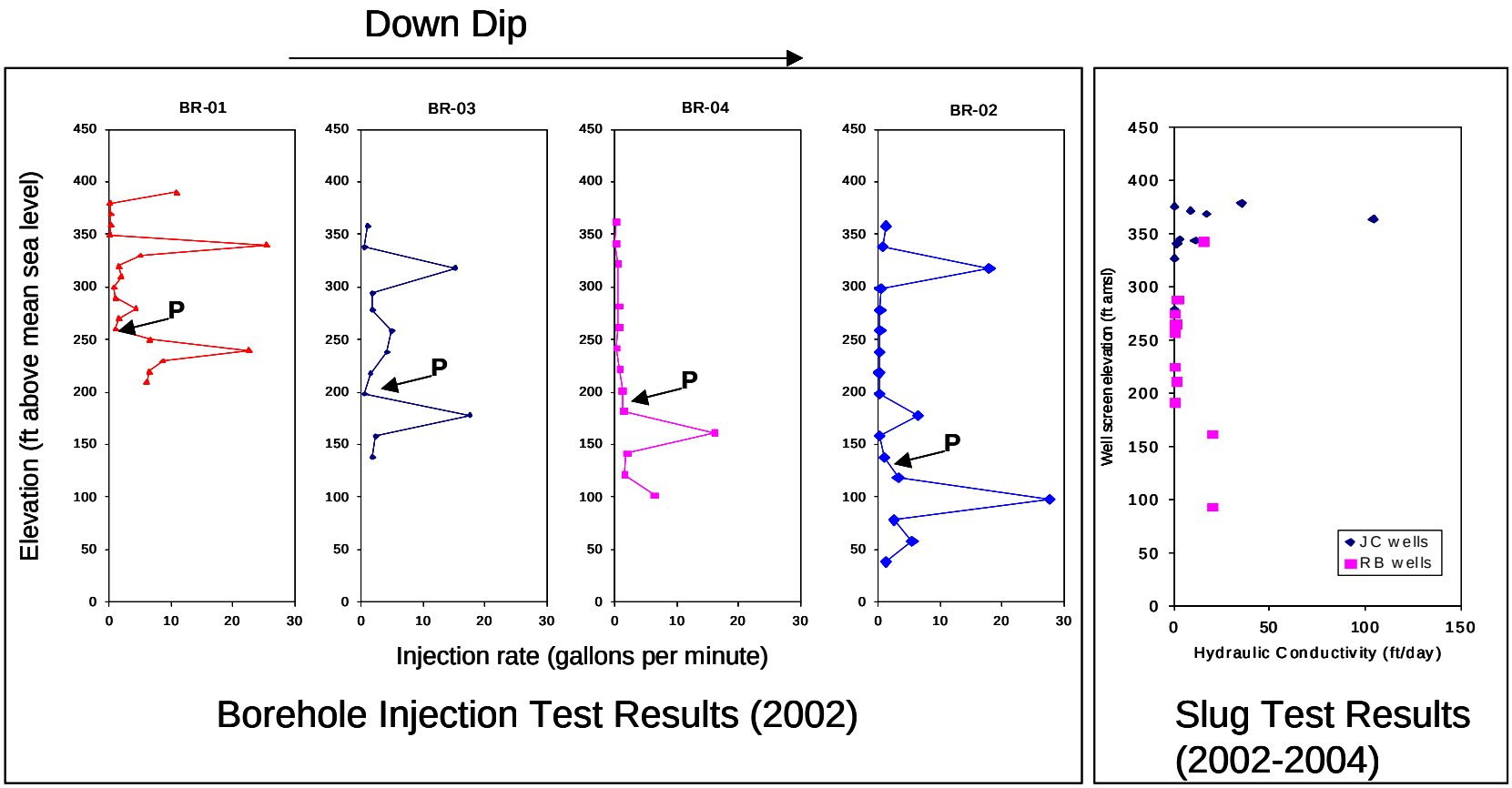


**Fig. 6. Borehole injection test results (LBG 2002) and hydraulic conductivities from slug testing in bedrock wells (LBG 2002, SAIC 2007). (Plane fitted through points marked "P" was used to define the upper boundary of the Roubidoux HSU layer.)**

Water Levels in Deep Overburden Wells Dec 2004

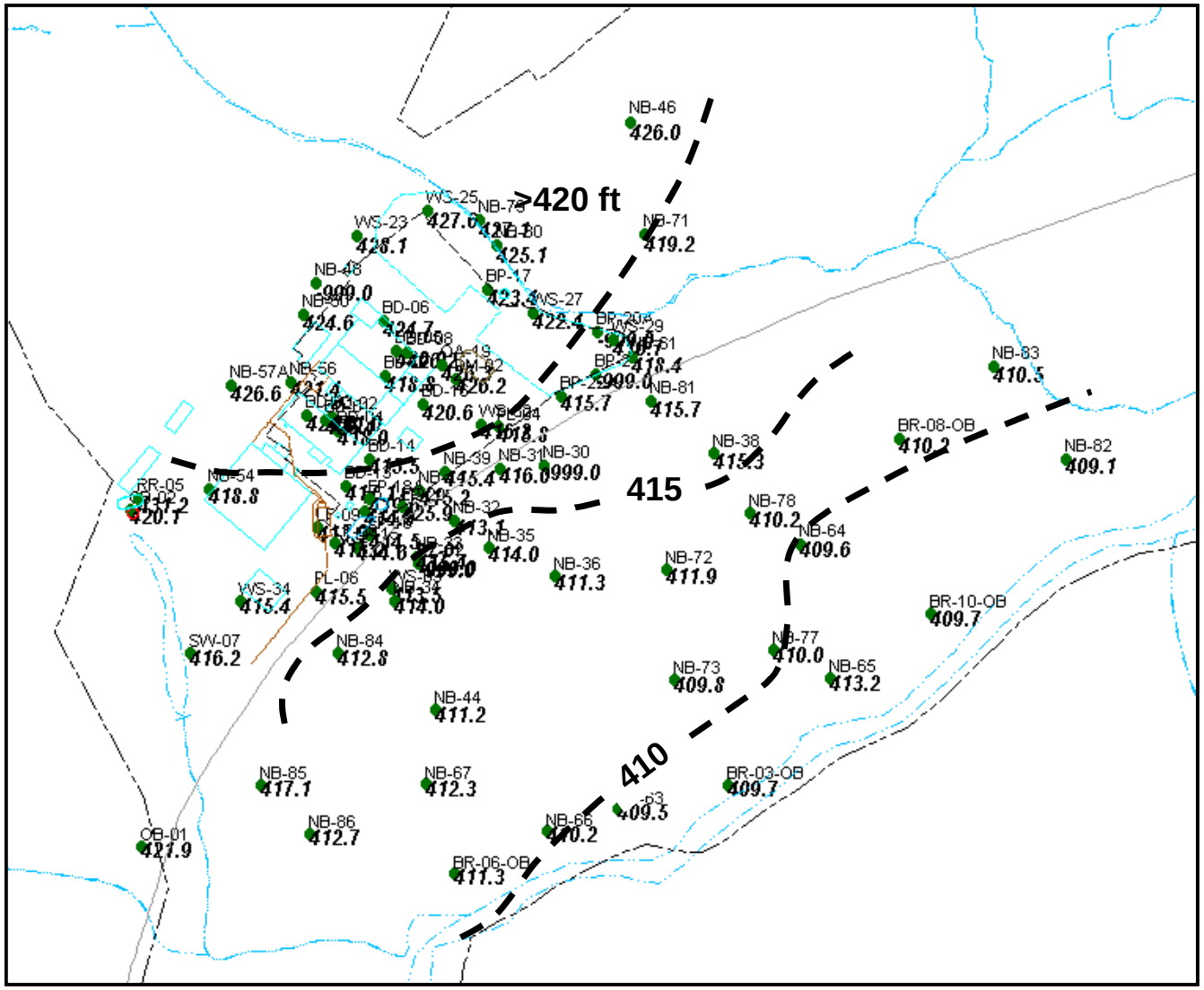


**Fig. 7. Potentiometric surface (ft above mean sea level) in the deep overburden (coarse-grain) hydrostratigraphic unit, December 2004.**

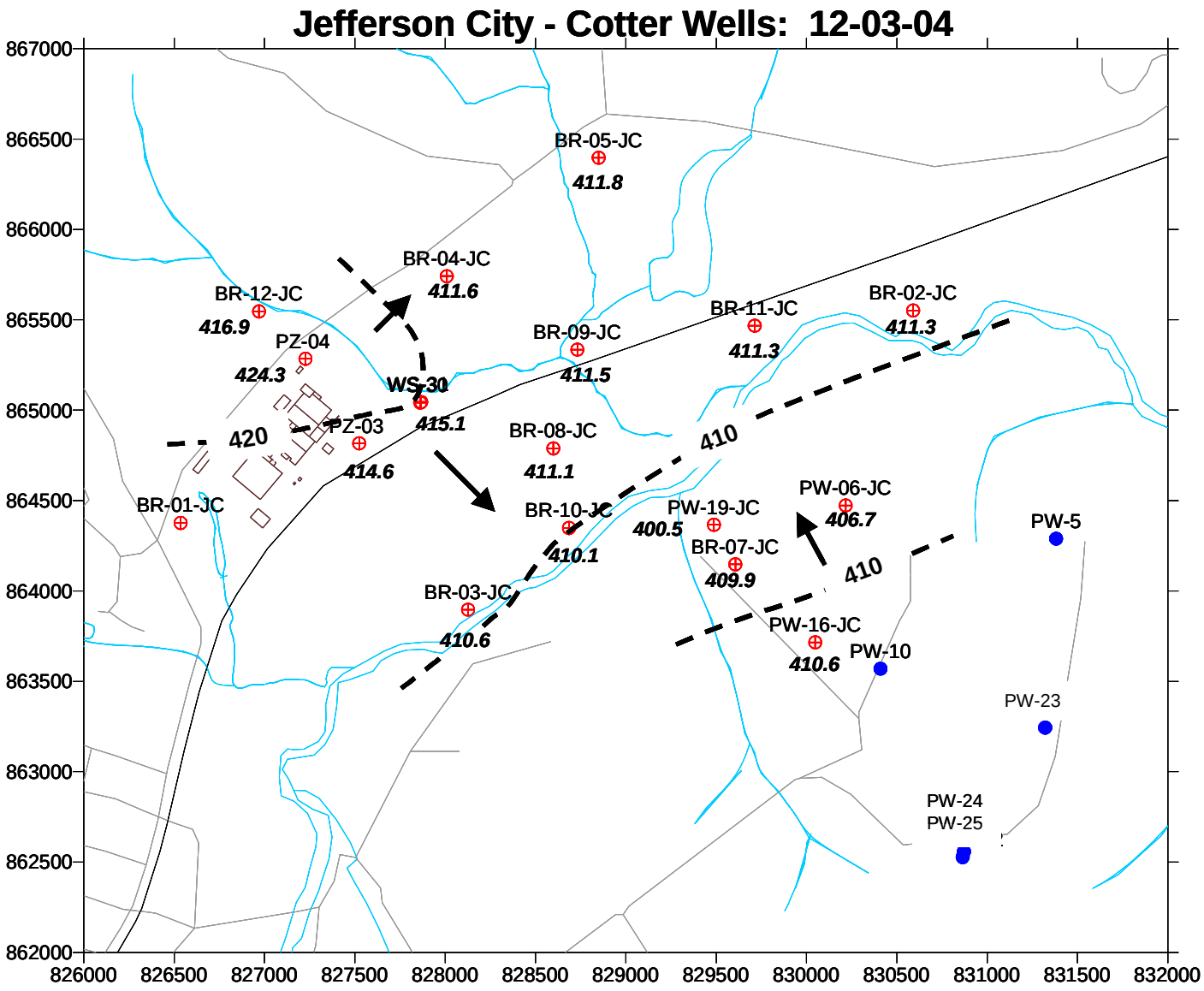


**Fig. 8. Potentiometric surface (ft above mean sea level) in the Jefferson City-Cotter hydrostratigraphic unit, December 2004.**

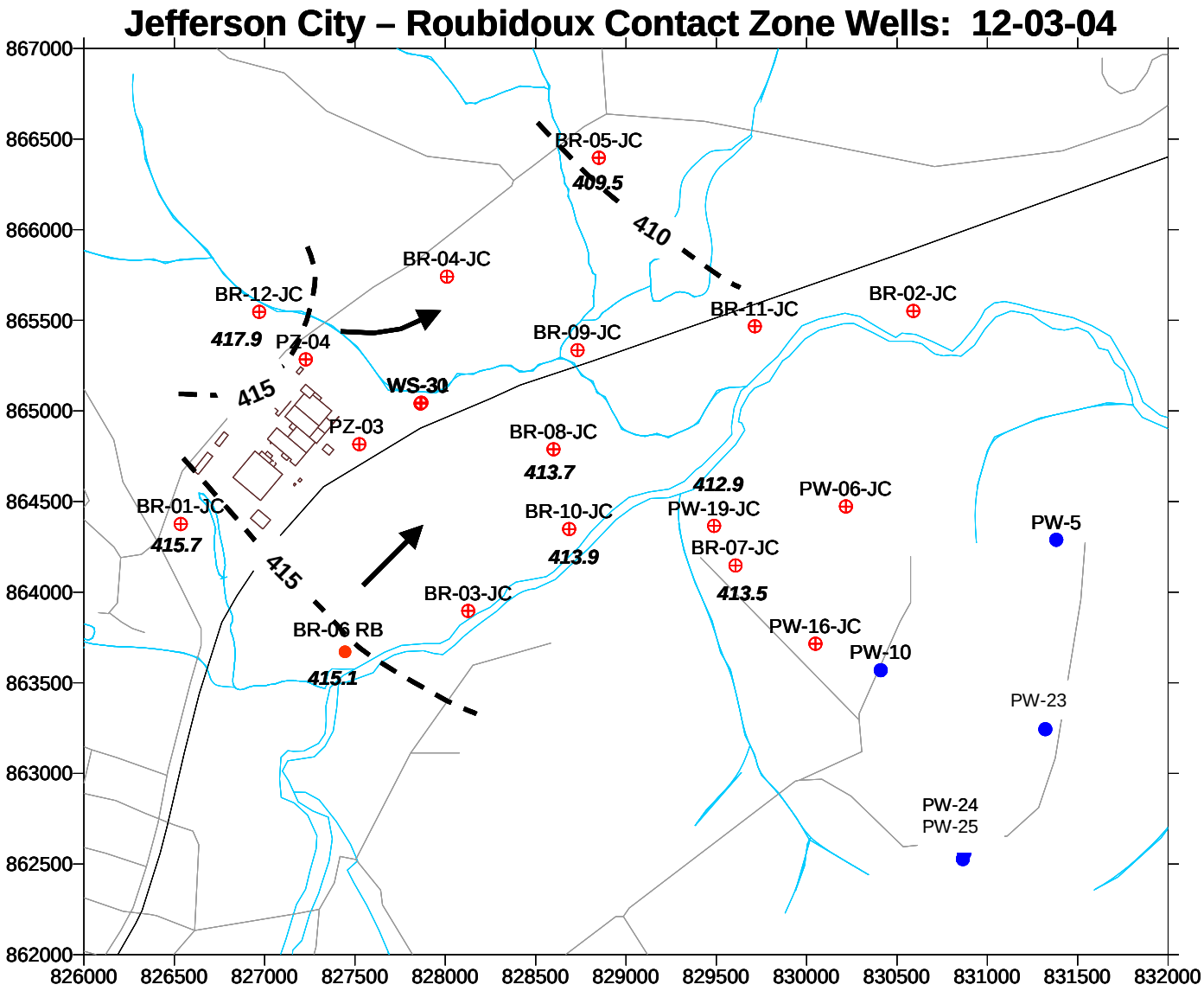


**Fig. 9. Potentiometric surface (ft above mean sea level) in the Jefferson City-Cotter-Roubidoux contact zone hydrostratigraphic unit, December 2004.**

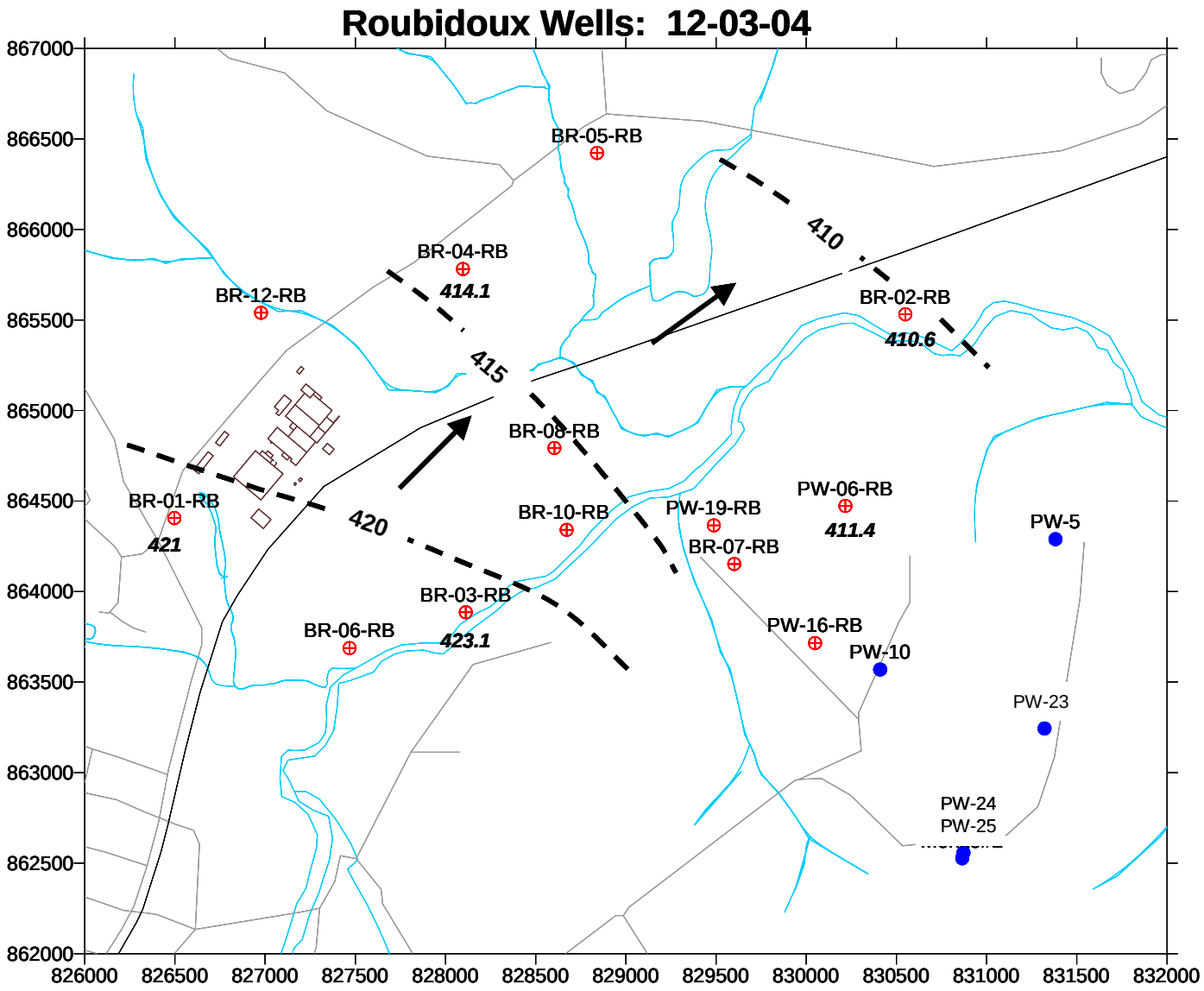


**Fig. 10. Potentiometric surface (ft above mean sea level) in the Roubidoux hydrostratigraphic unit, December 2004.**

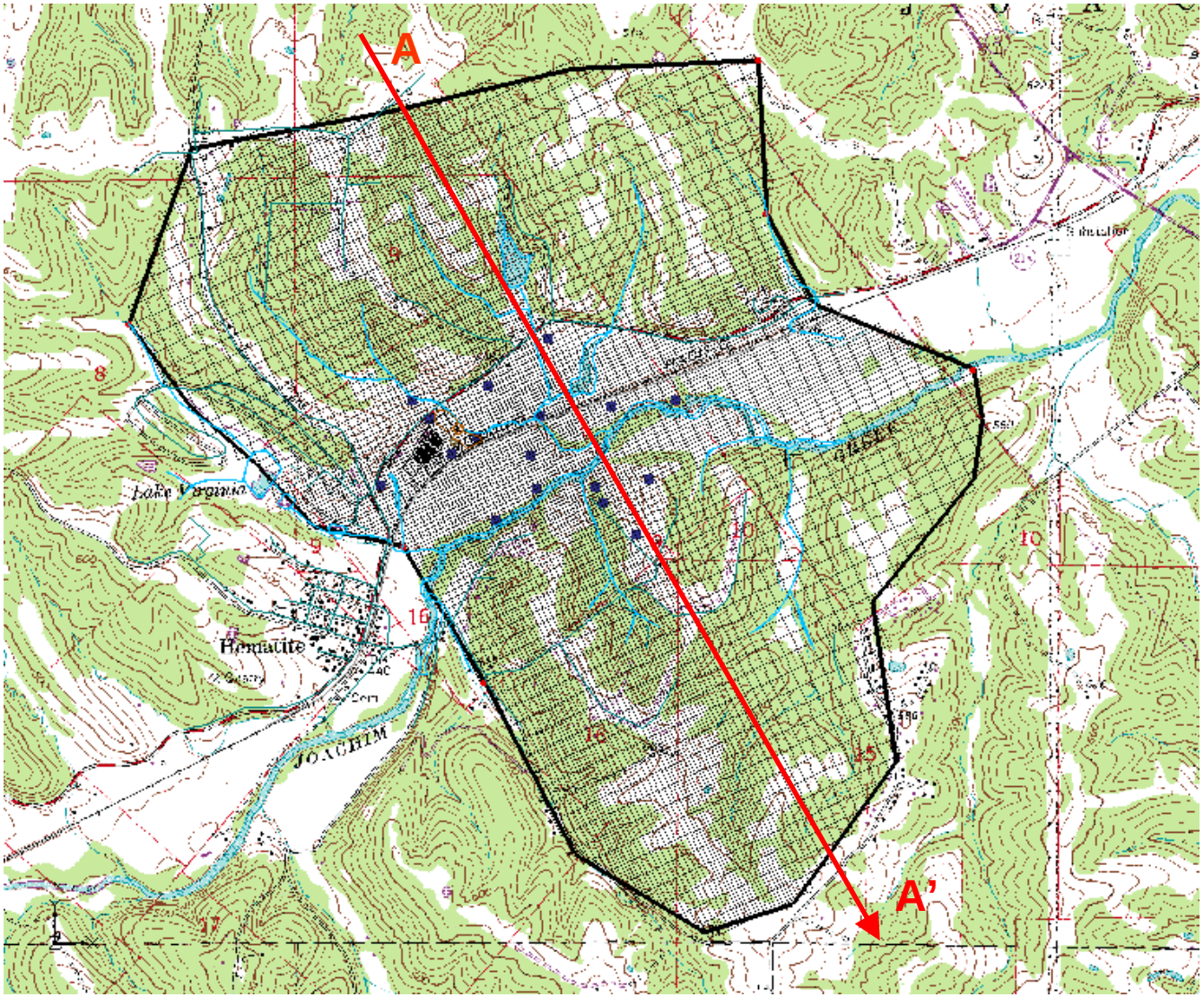


**Fig. 11. Plan view of MODFLOW/RT3D model domain for the Hematite Site, bounded by solid black line. [Model grid also shown; blue dots correspond to bedrock well locations; Line A-A' corresponds to the cross-section shown in Fig. 14.)]**

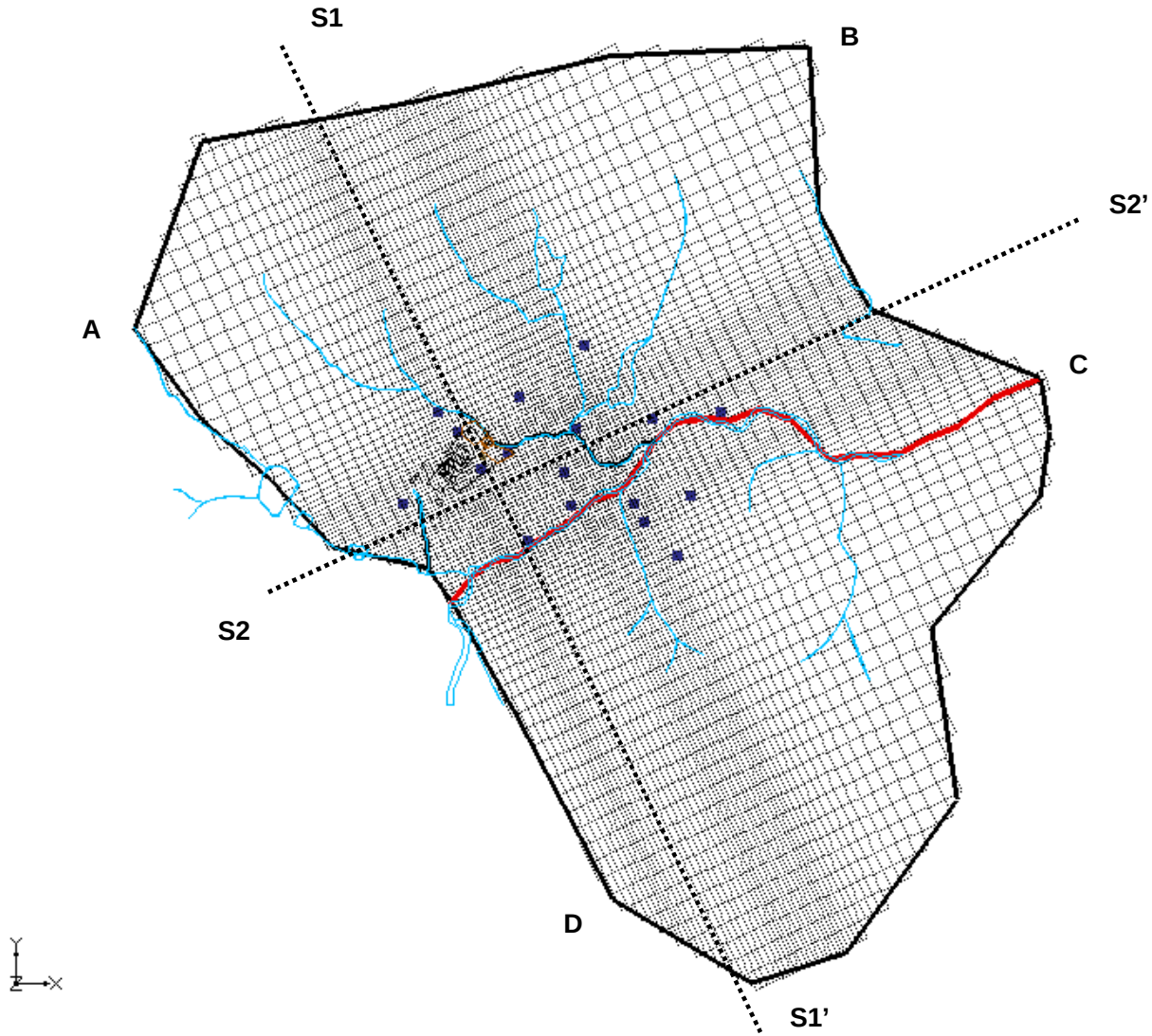


**Fig. 12. Plan view of model grid. [The red line corresponds to Joachim Creek; grid cells in Layer 1 that lie along this line are specified head cells; arcs A-D and B-C are specified head arcs in Layers 8 and 9 (see text for more details); Lines S1-S1' and S2-S2' correspond to cross-sections of model grid shown in Figs. 13 and 14, respectively.)]**

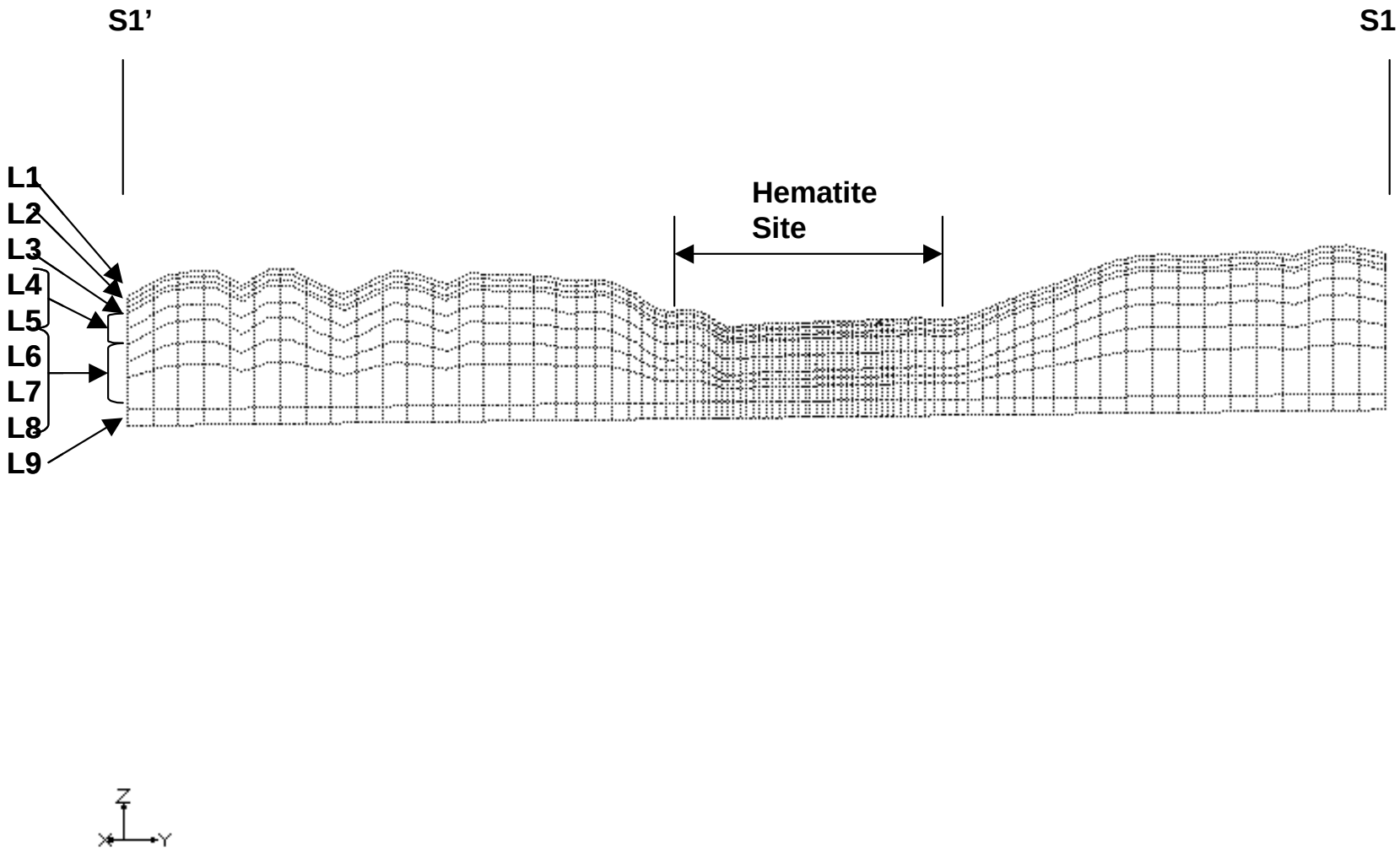


**Fig. 13. Elevation view of model grids facing southwest. (Refer to Fig. 12 for orientation of cross-section.)**

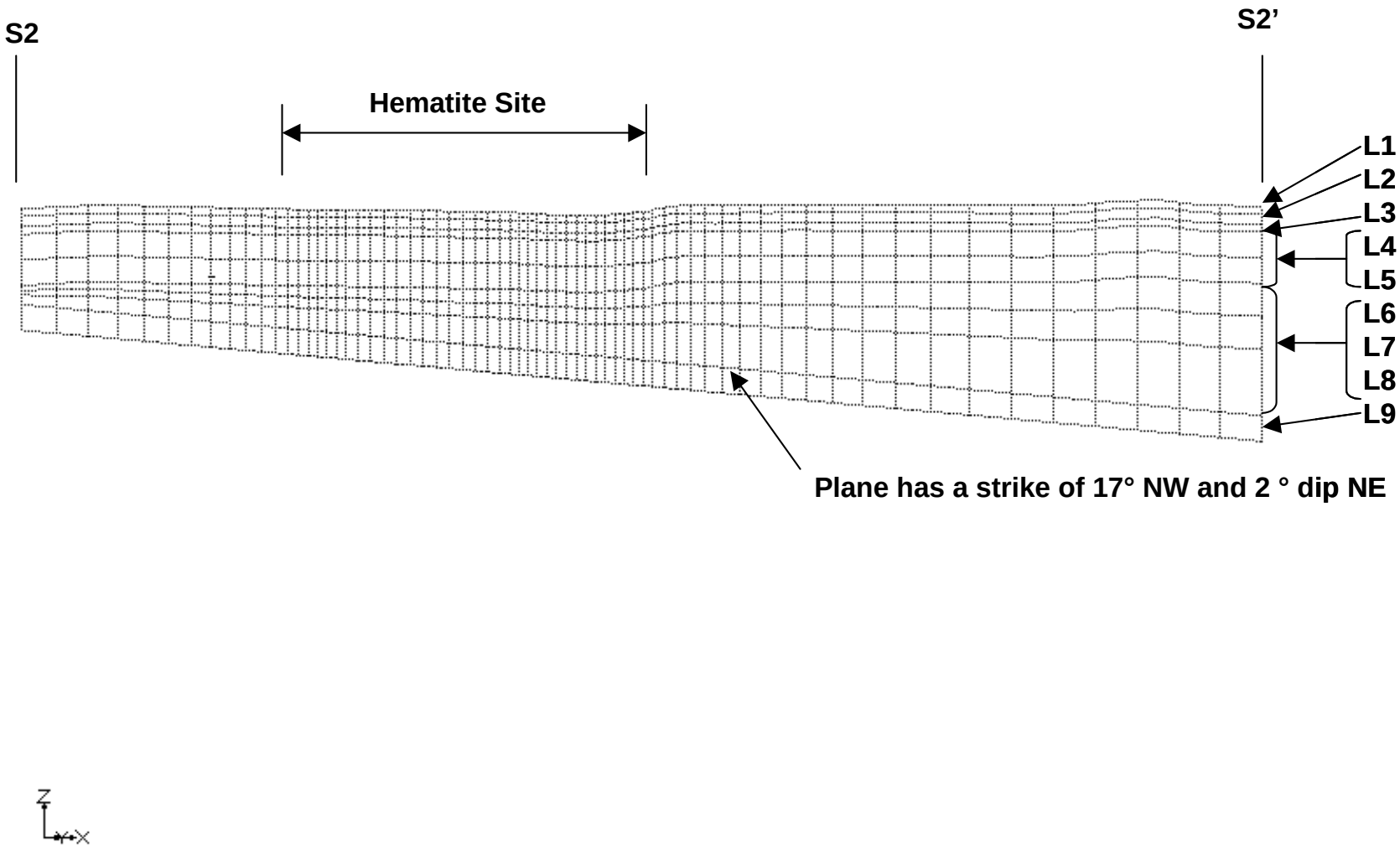


**Fig. 14. Elevation view of model grid, looking northwest (Refer to Fig. 12 for orientation of cross-section.)**

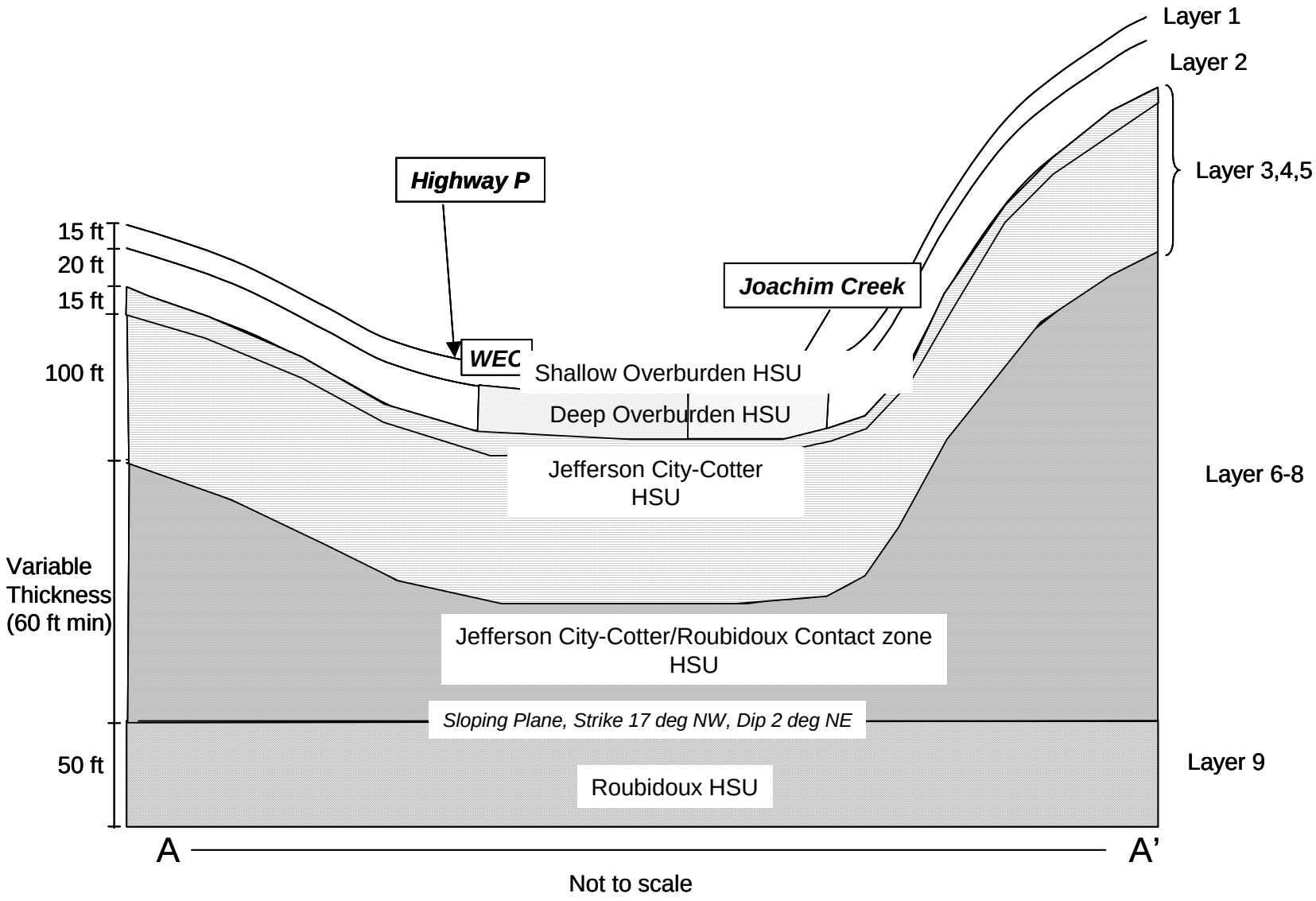


**Fig. 15. Hydrostratigraphic units and corresponding layers represented in MODFLOW model. (Cross-section A-A' in Fig. 11, trending northwest-southeast.)**

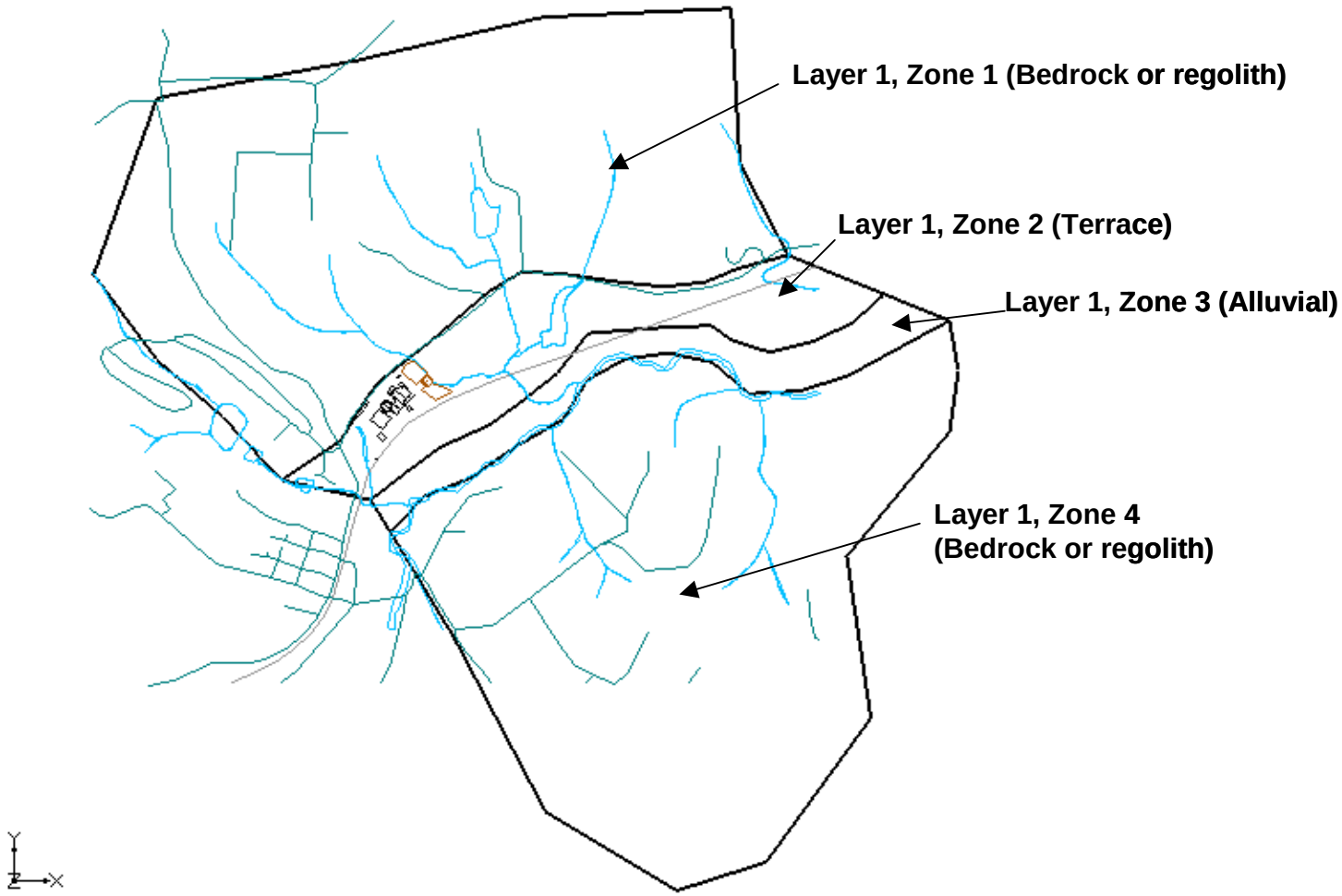


**Fig. 16. Constant property zones within Layer 1. (Zone 1 and Zone 4 correspond to bedrock in the highlands on either side of Joachim Creek Valley; Zone 2 corresponds to the thick, fine-grained sediments in the terrace deposits; Zone 3 corresponds to the thinner, fine-grained deposits in the alluvial sediments.)**

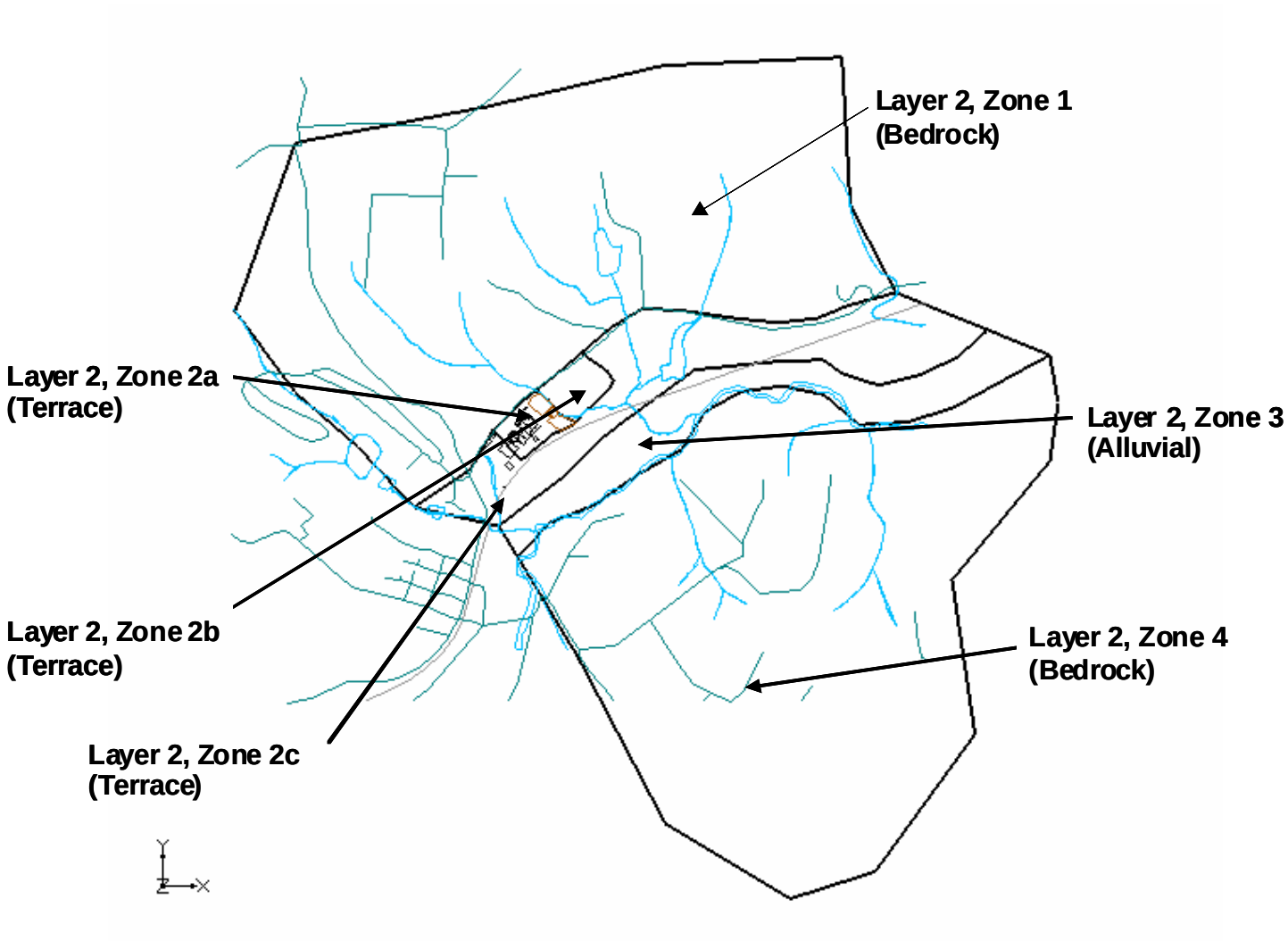


**Fig. 17. Constant property zones within Layer 2. (Zone 1 and Zone 4 correspond to bedrock in the highlands on either side of Joachim Creek Valley; Zone 2 corresponds to the thicker, fine-grained sediments in the terrace deposits; Zone 3 corresponds to the thinner, fine-grained deposits in the alluvial sediments.; refer to the text for a description of Zones 2a, 2b and 2c.)**

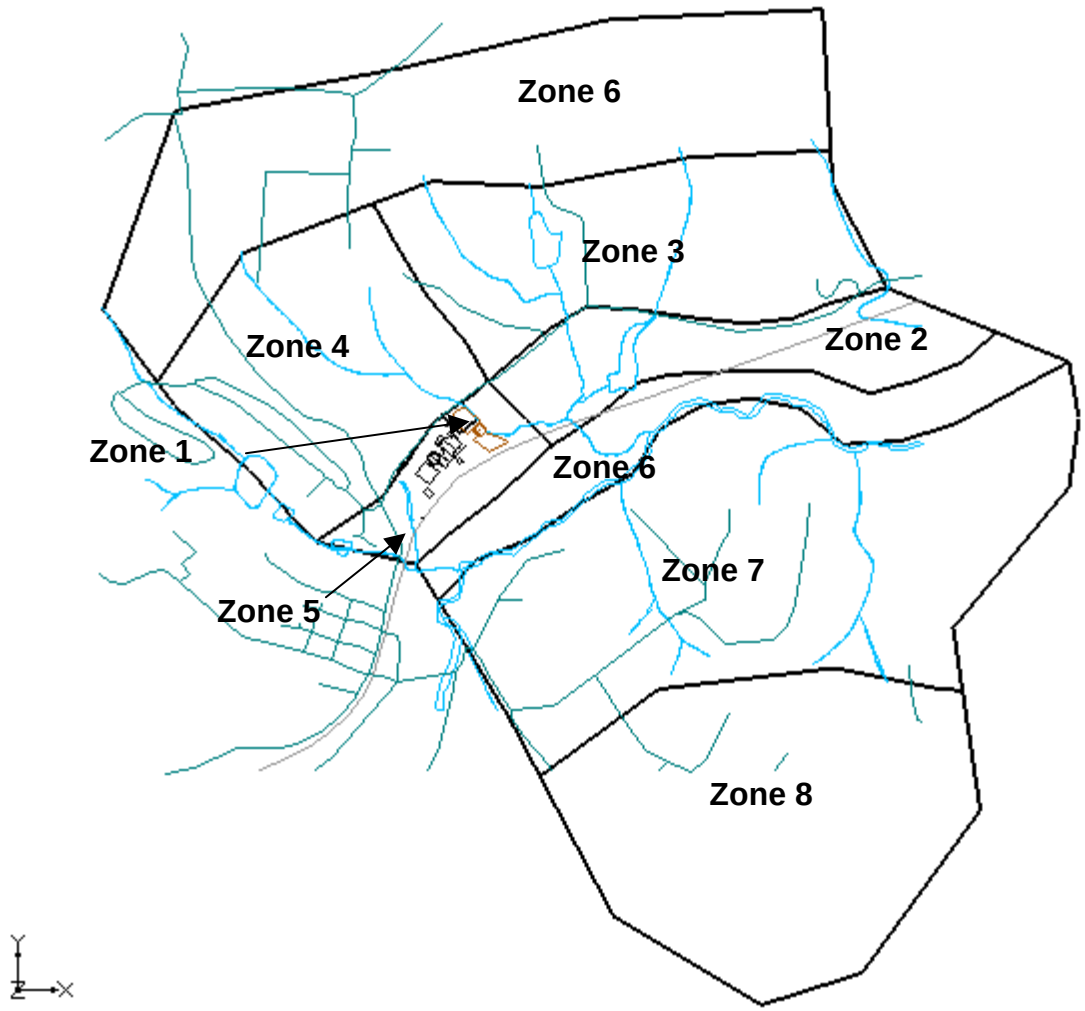


**Fig. 18. Recharge zones for the Hematite Site MODFLOW mode.**

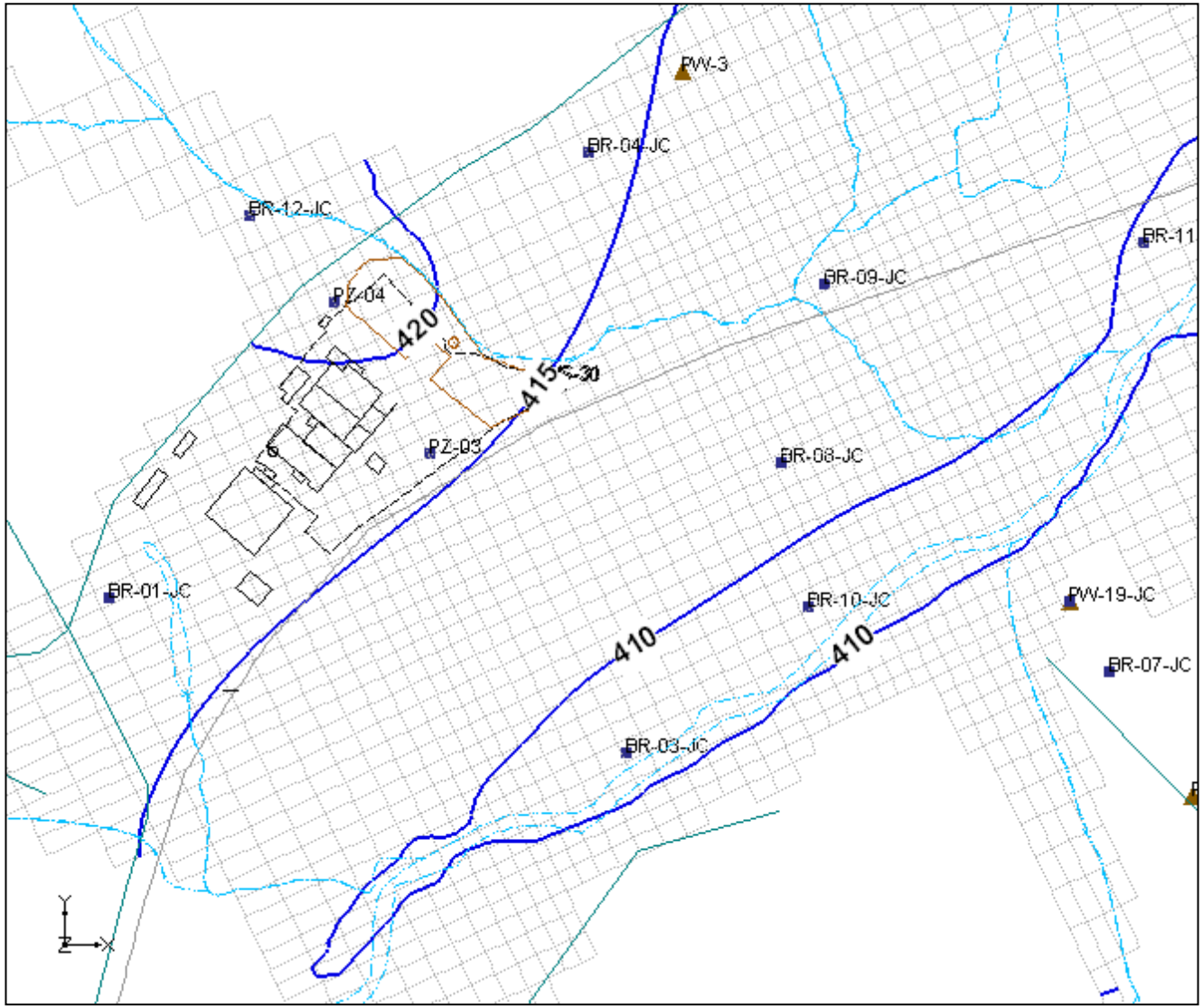


**Fig. 19. Potentiometric surface (ft above mean sea level) in Layer 2 of calibrated steady-state MODFLOW model. (Layer 2 corresponds to the deep overburden HSU.)**

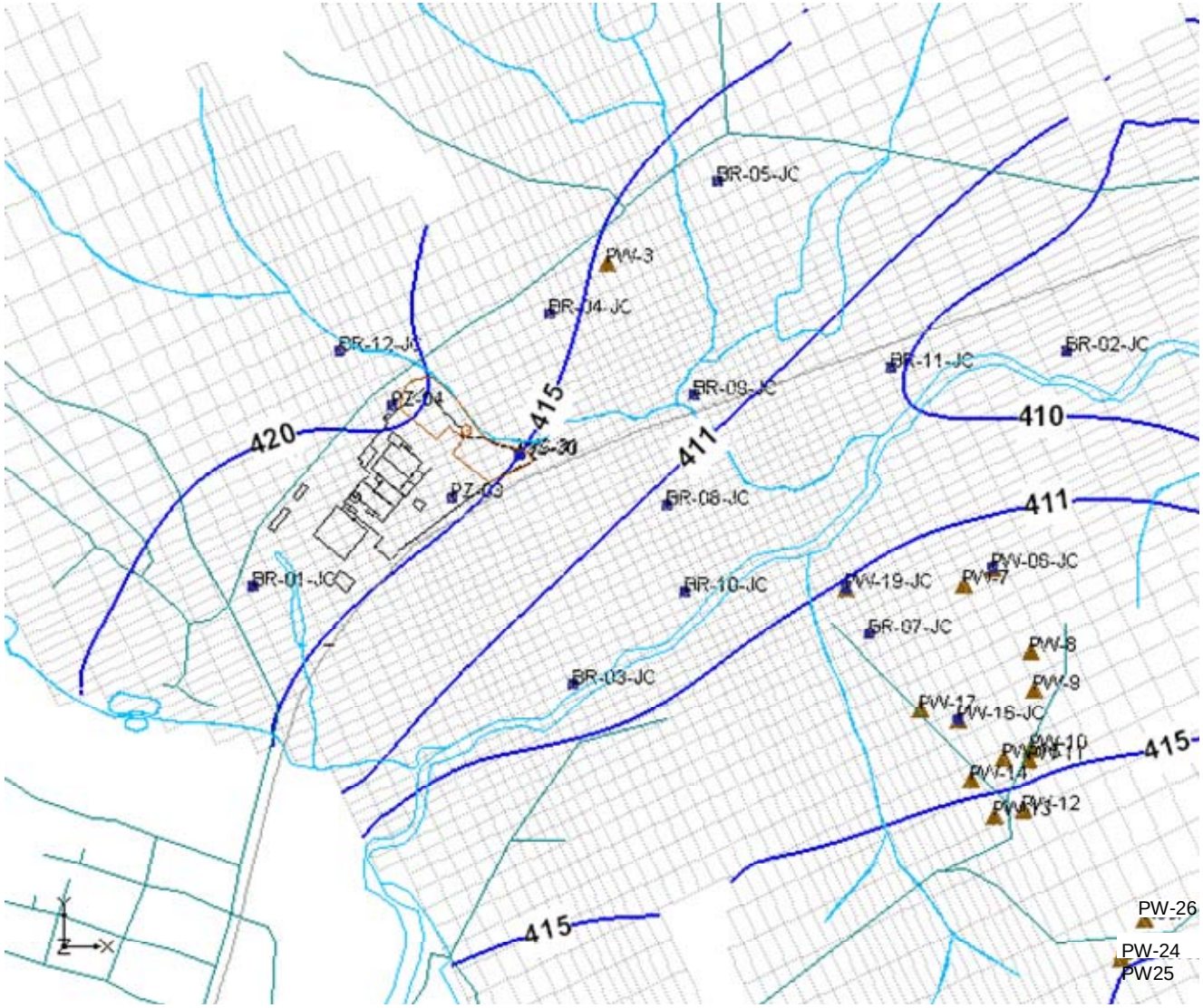


**Fig. 20. Potentiometric surface (ft above mean sea level) in Layer 5 of calibrated steady-state MODFLOW model. (Layer 5 corresponds to the Jefferson-City Cotter HSU.)**

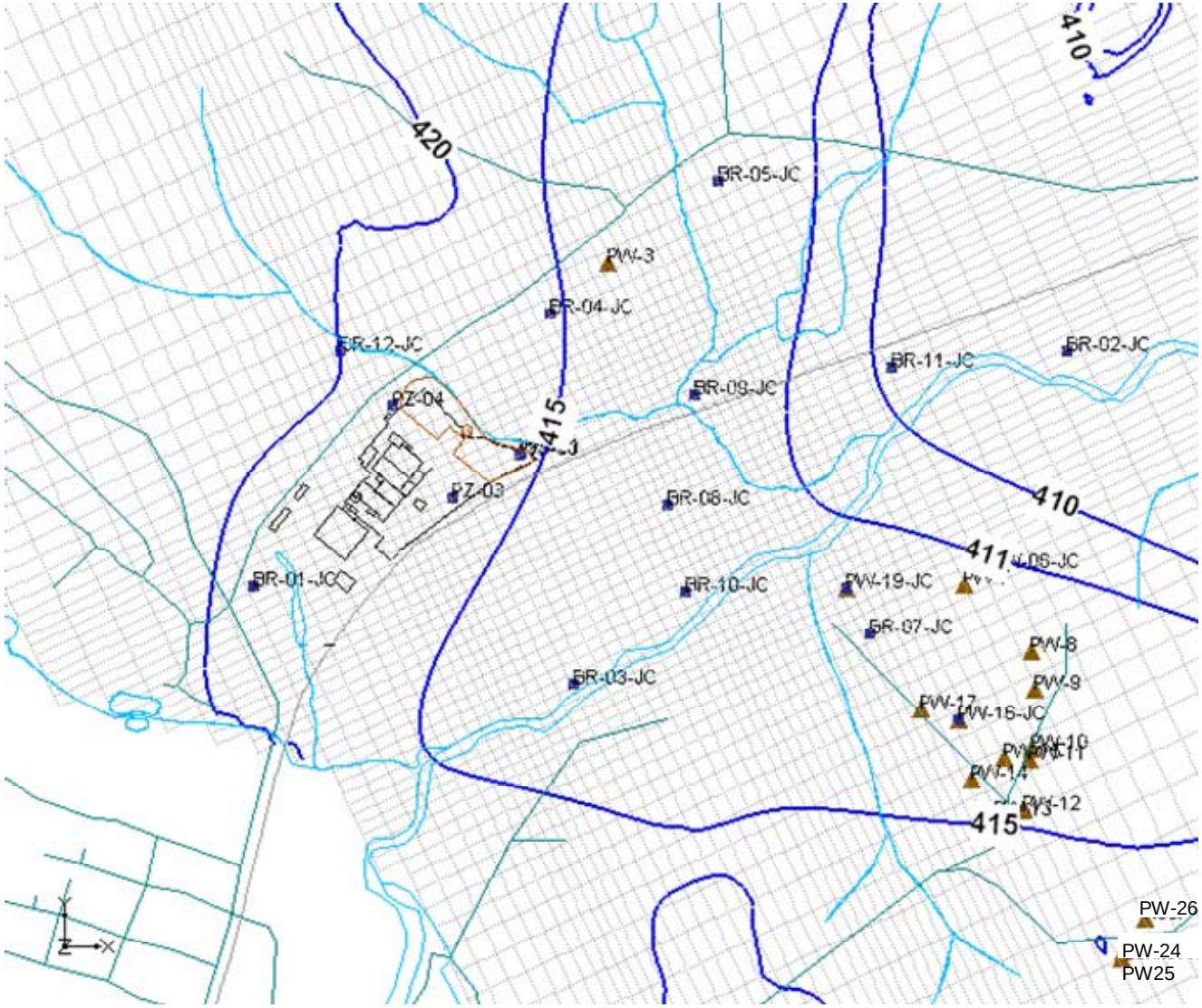


**Fig. 21. Potentiometric surface (ft above mean sea level) in Layer 8 of calibrated steady-state MODFLOW model. (Layer 8 corresponds to the Jefferson-City Cotter/Roubidoux contact zone HSU.)**

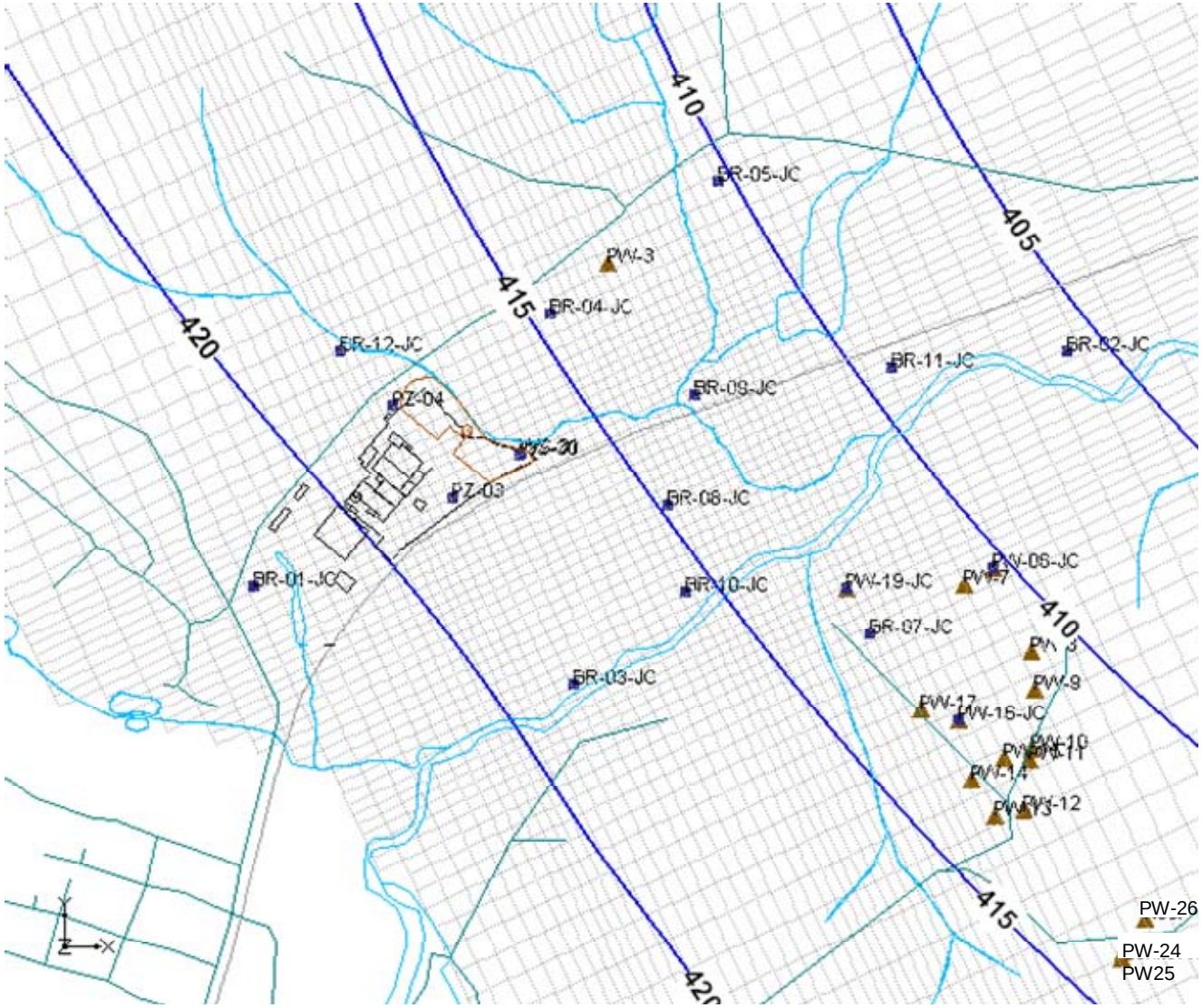


**Fig. 22. Potentiometric surface (ft above mean sea level) in Layer 9 of calibrated steady-state MODFLOW model. (Layer 9 corresponds to the Jefferson-City Cotter/Roubidoux contact zone HSU.)**

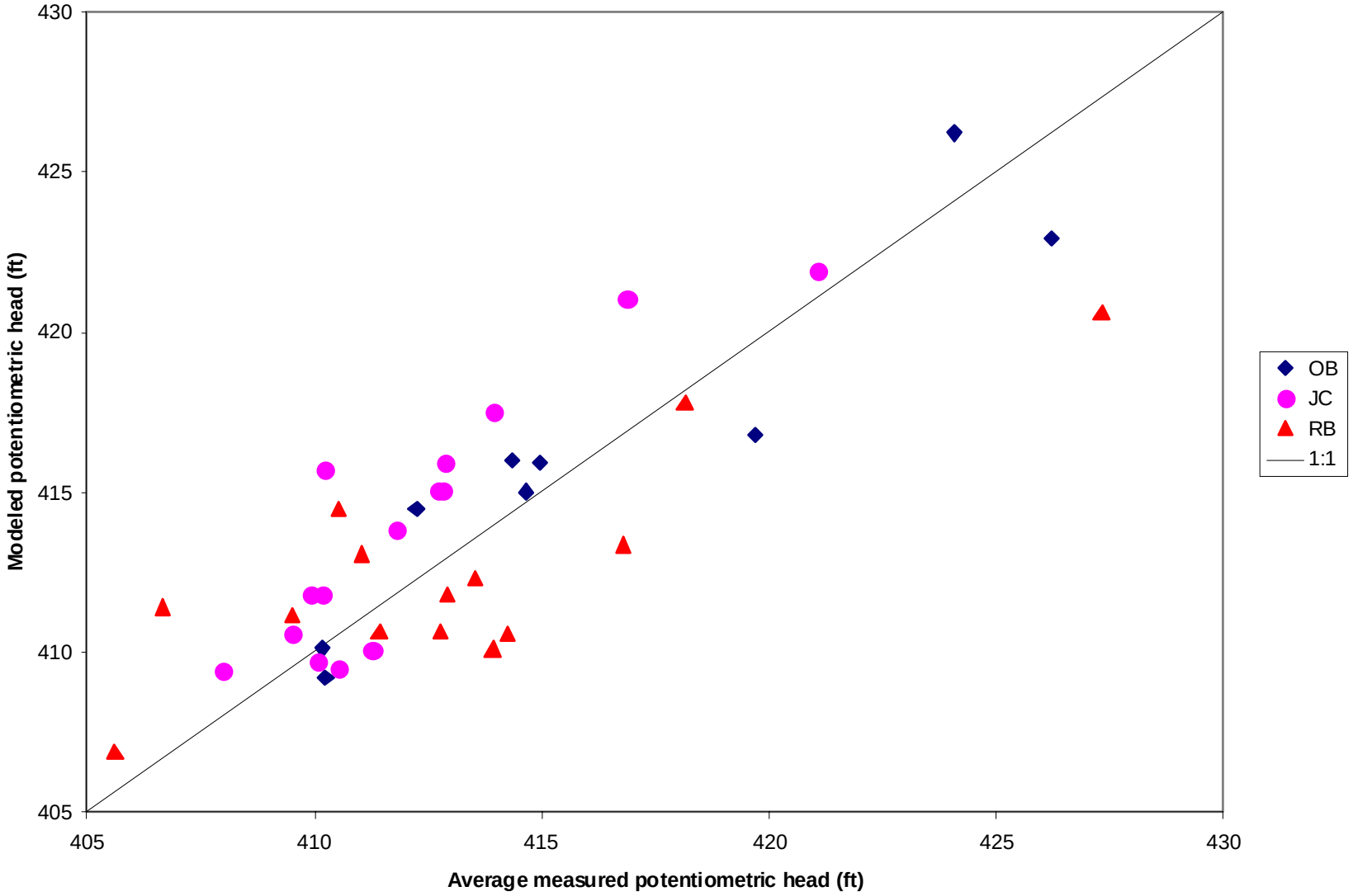


**Fig. 23. Comparison between modeled and average measured water levels in wells at the Hematite Site. (Deep overburden (OB), Jefferson City-Cotter (JC), and Roubidoux (RB) wells; see the text for a residual summary.)**

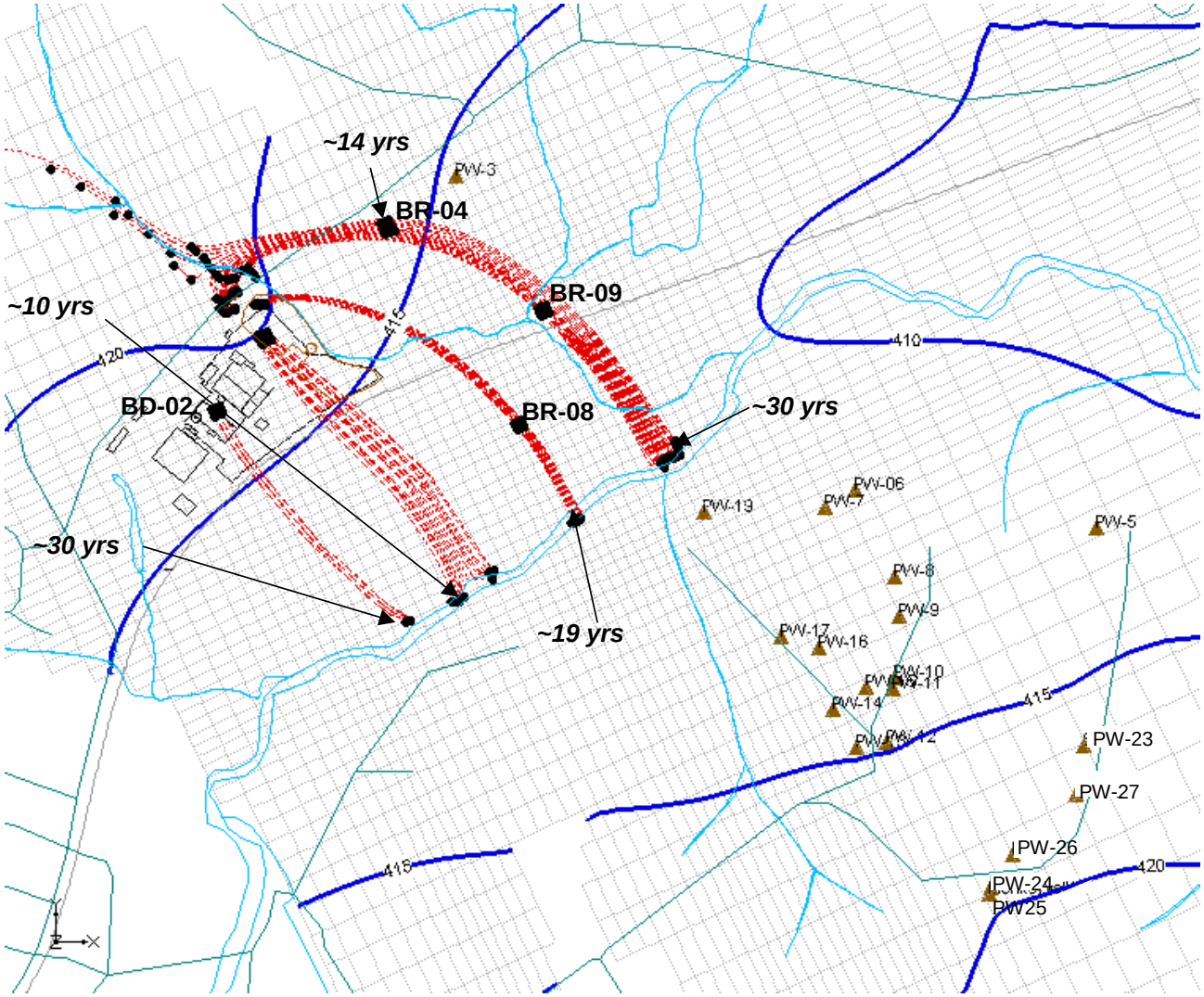


**Fig. 24. MODPATH-simulated (forward and backward) particle pathways and travel times. [Blue lines are potentiometric contour lines for layer corresponding to transmissive Jefferson City-Cotter HSU; pumping in private wells at household rates (35 $ft^3$/day).].** ***Note that particle pathways indicate groundwater flowlines and are not necessarily contaminant pathways.***

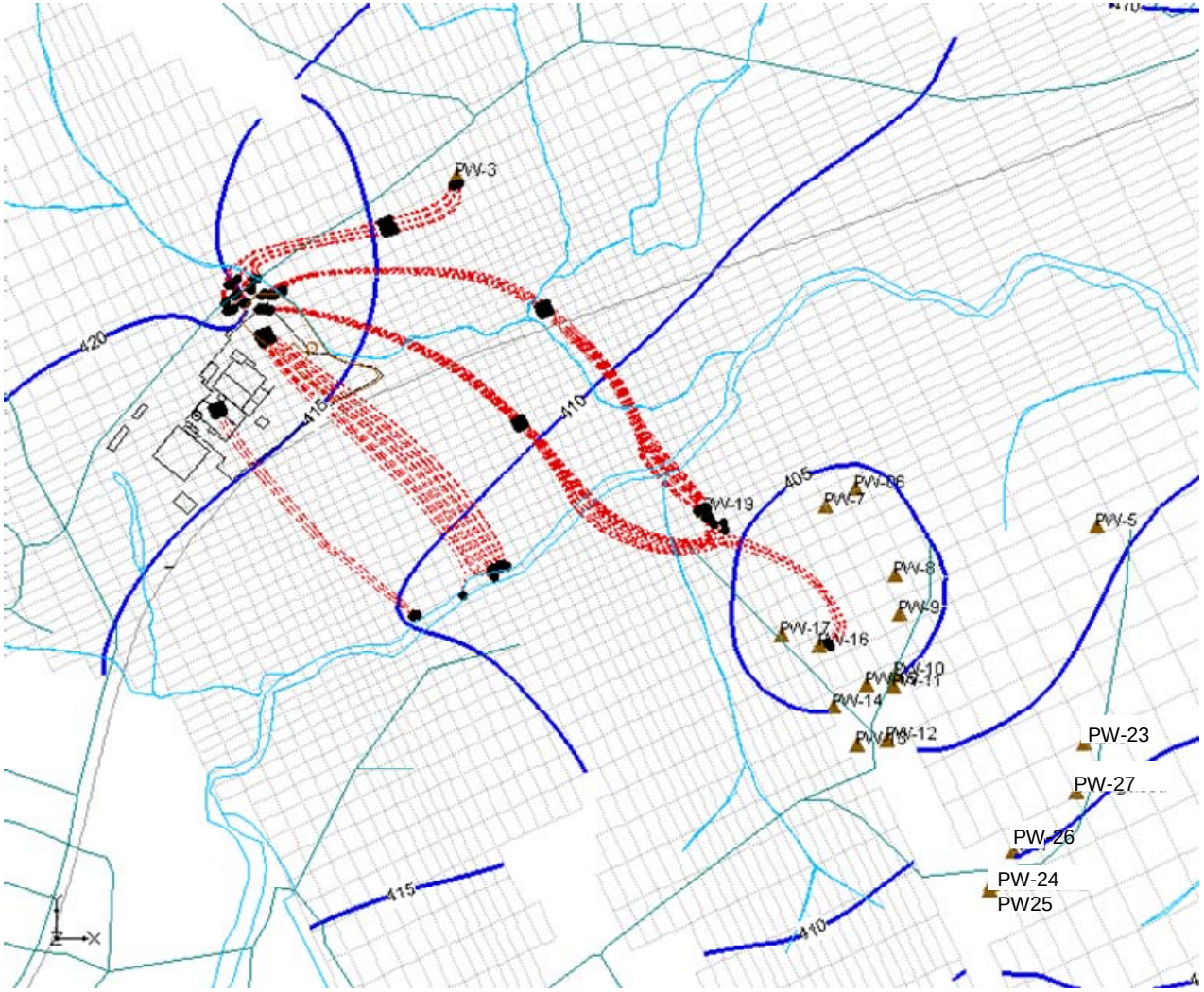


**Fig. 25. MODPATH-simulated (forward and backward) particle pathways and travel times. [Blue lines are potentiometric contour lines for layer corresponding to Jefferson City-Cotter HSU; specified extraction flow rate in private wells at 2000 ft$^3$/day (~10.4 gpm) drawn from Jefferson City-Cotter HSU layer to simulate vertical borehole flow.)** ***Note that particle pathways indicate groundwater flowlines and are not necessarily contaminant pathways.***

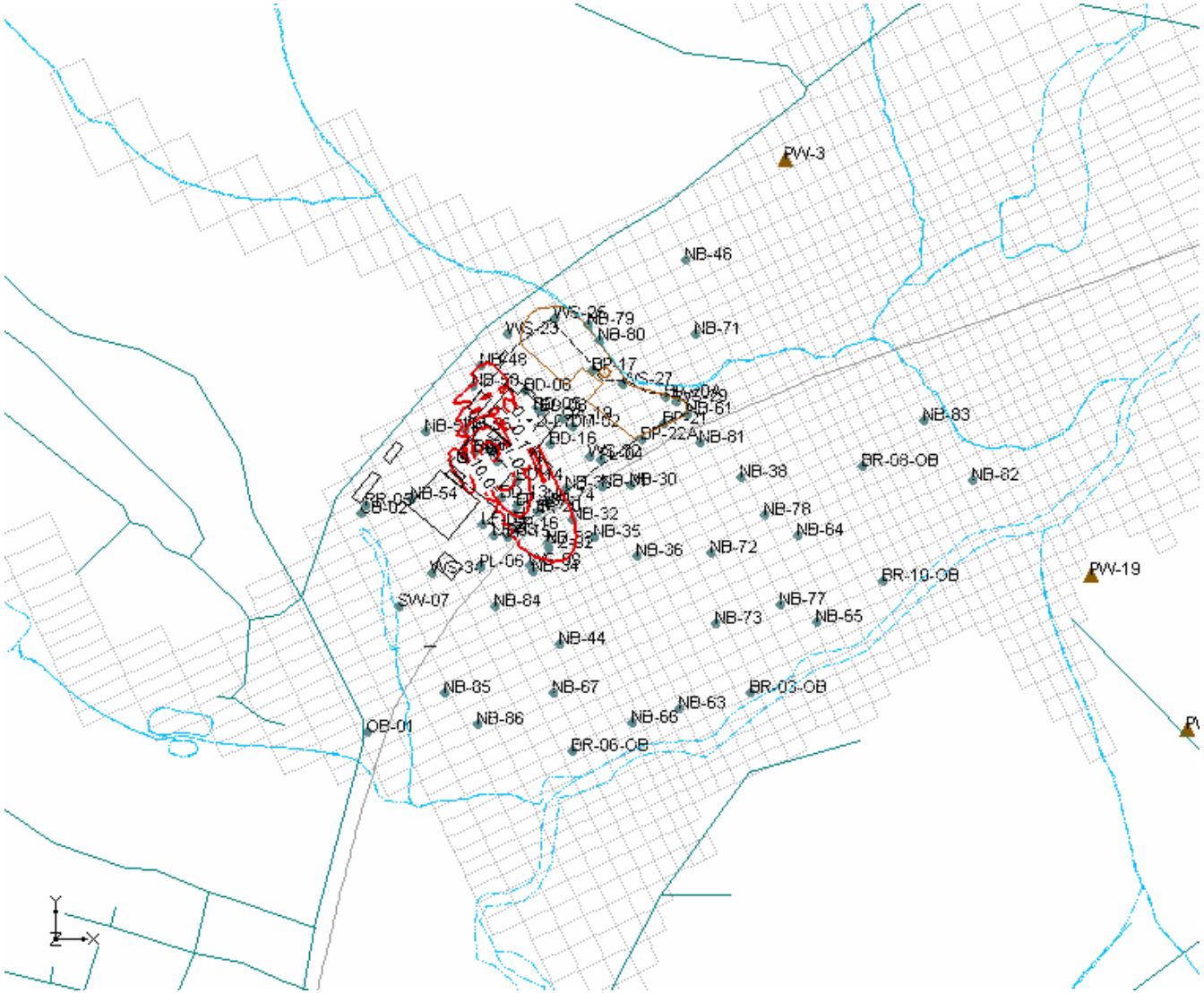


**Fig. 26. Simulated PCE concentration contours (mg/L) in layer corresponding to terrace/alluvial deposits at t = 3000 days (~8 years). (Constant concentration source of 200 mg/L PCE placed in cell corresponding to BD-02; simulated using MODFLOW model with vertical borehole flow and RT3D Sequential Decay chemical reaction package.)**

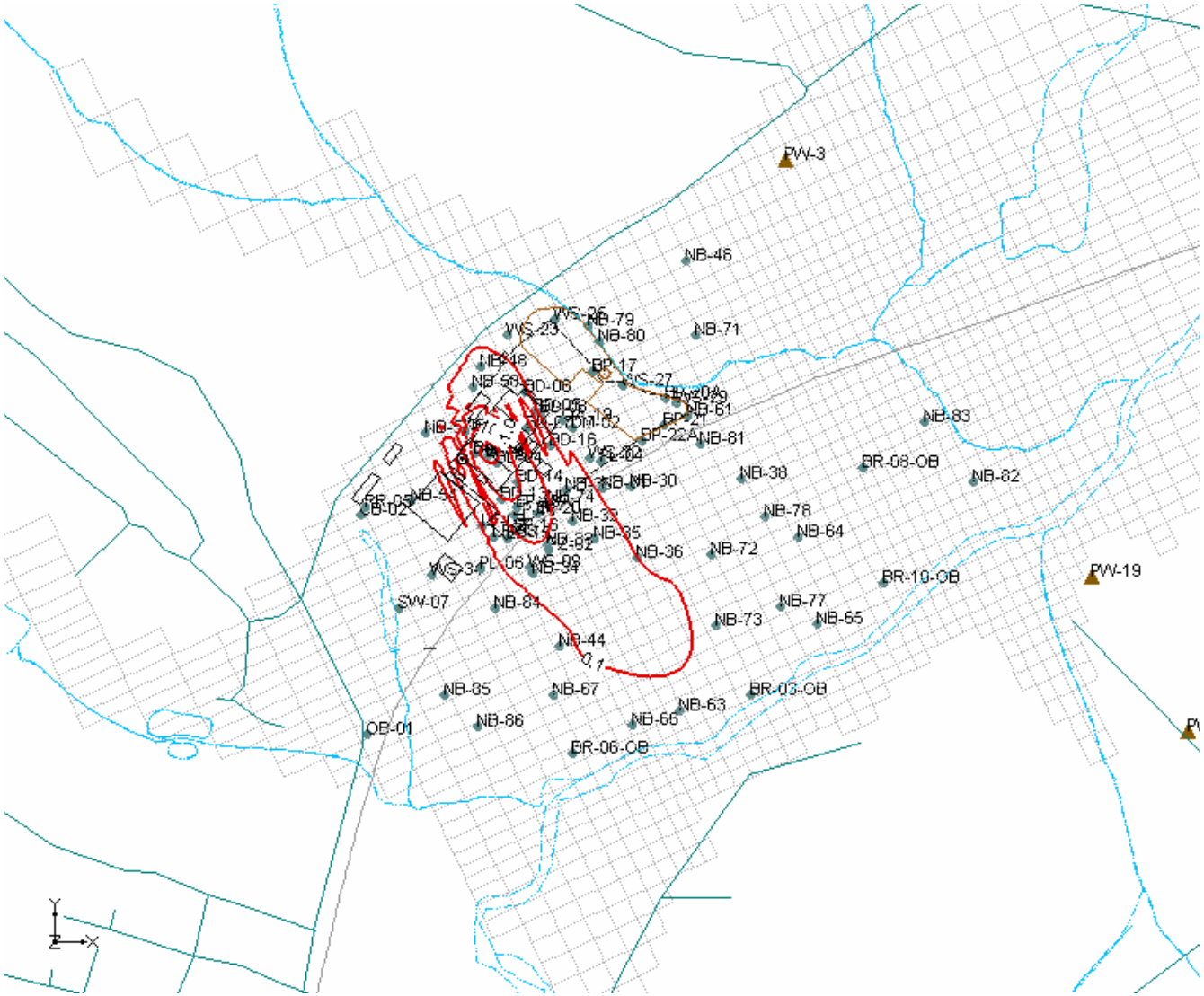


**Fig. 27. Simulated PCE concentration contours (mg/L) in layer corresponding to terrace/alluvial deposits at t = 9000 days (~25 years). (Constant concentration source of 200 mg/L PCE placed in cell corresponding to BD-02; simulated using MODFLOW model with vertical borehole flow and RT3D Sequential Decay chemical reaction package.)**

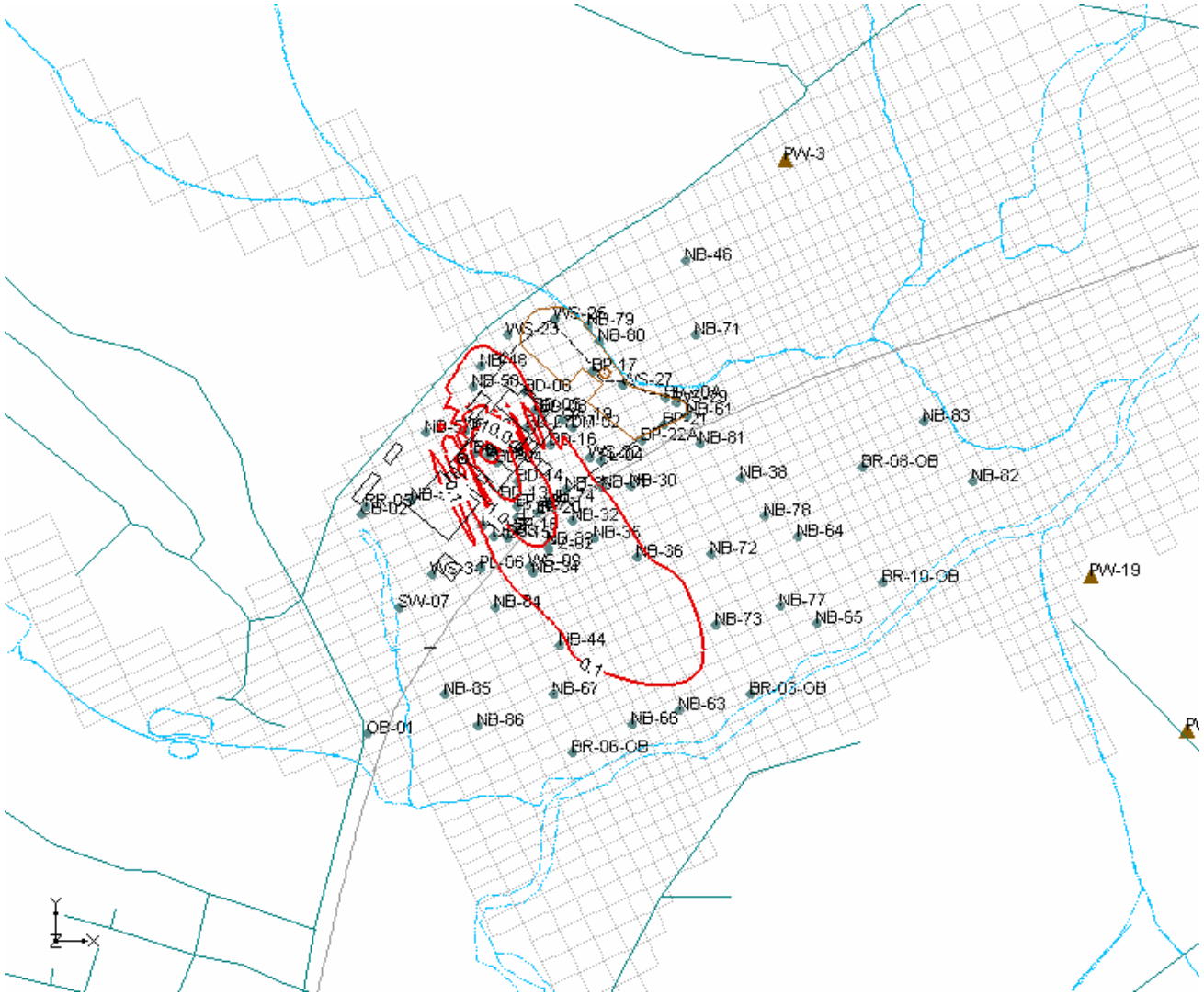


**Fig. 28. Simulated PCE concentration contours (mg/L) in layer corresponding to terrace/alluvial deposits at t = 15,000 days (~41 years). [Constant concentration source of 200 mg/L PCE placed in cell corresponding to BD-02; simulated using MODFLOW model with vertical borehole flow and RT3D Sequential Decay chemical reaction package; note that there is not much difference when compared to t = 9000 days (Fig. 28); suggests steady-state conditions in contaminant distribution.]**

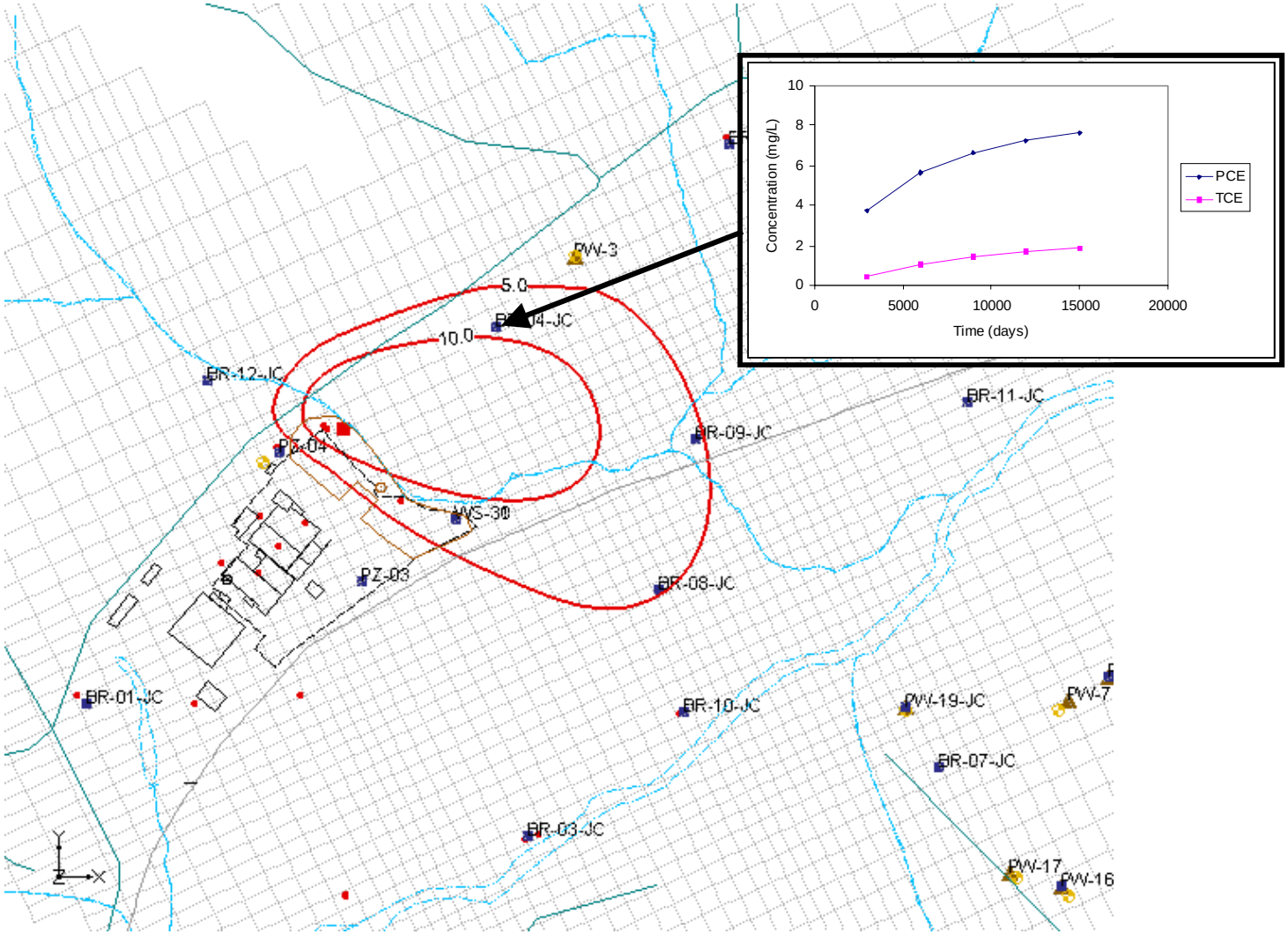


**Fig. 29. Simulated PCE concentration contours (mg/L) in layer corresponding to transmissive Jefferson City-Cotter Formation at t = 15,000 days (~41 years). [Constant concentration source of 100 mg/L PCE placed in Burial Pits (red square); simulated using MODFLOW model with vertical borehole flow and RT3D sequential decay chemical reaction package (PCE > TCE > *cis*-1,2-DCE > vinyl chloride > ethene); inset graph shows PCE and TCE concentrations versus time at location corresponding to BR-04-JC.]**

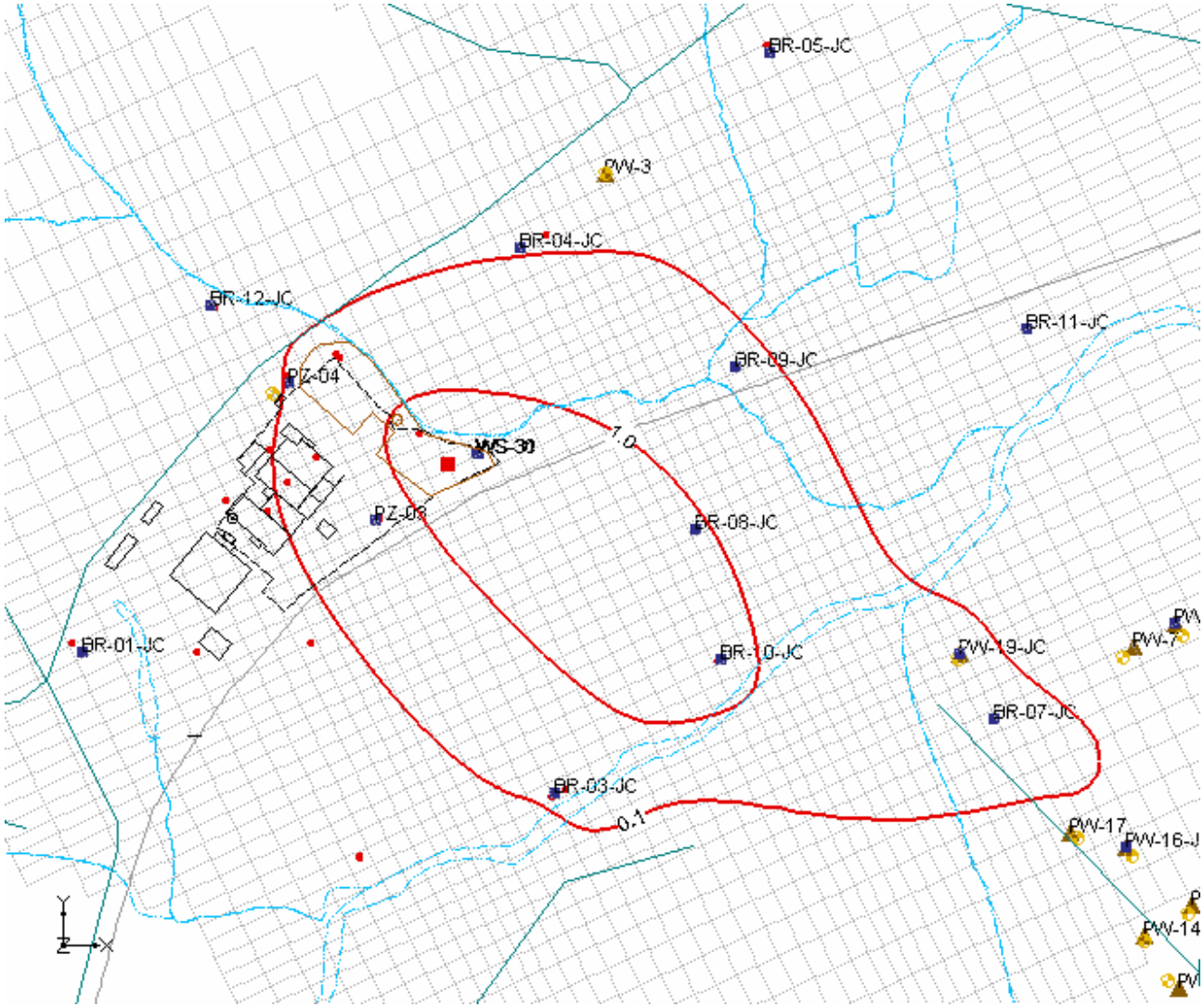


**Fig. 30. Simulated TCE concentration contours (mg/L) in layer corresponding to transmissive Jefferson City-Cotter Formation at t = 15,000 days (~41 years). [Constant concentration source of 50 mg/L PCE and 50 mg/L TCE placed in vicinity of Burial Pits (red square); simulated using MODFLOW model with vertical borehole flow and RT3D sequential decay chemical reaction package (PCE > TCE > *cis*-1,2-DCE > vinyl chloride > ethene); note that TCE shown in figure is from degradation of PCE in source.]**

**Fig. 31. Simulated uranium concentration contours (mg/L) in layer corresponding to deep overburden at t = 74,000 days (~200 years). [Constant concentration source of 0.2 mg/L uranium placed in Burial Pits and Deul's Mountain (red squares); simulated using MODFLOW model with vertical borehole flow and RT3D Tracer Transport package (includes partition coefficient measured in site-specific study (SAIC 2003).]**

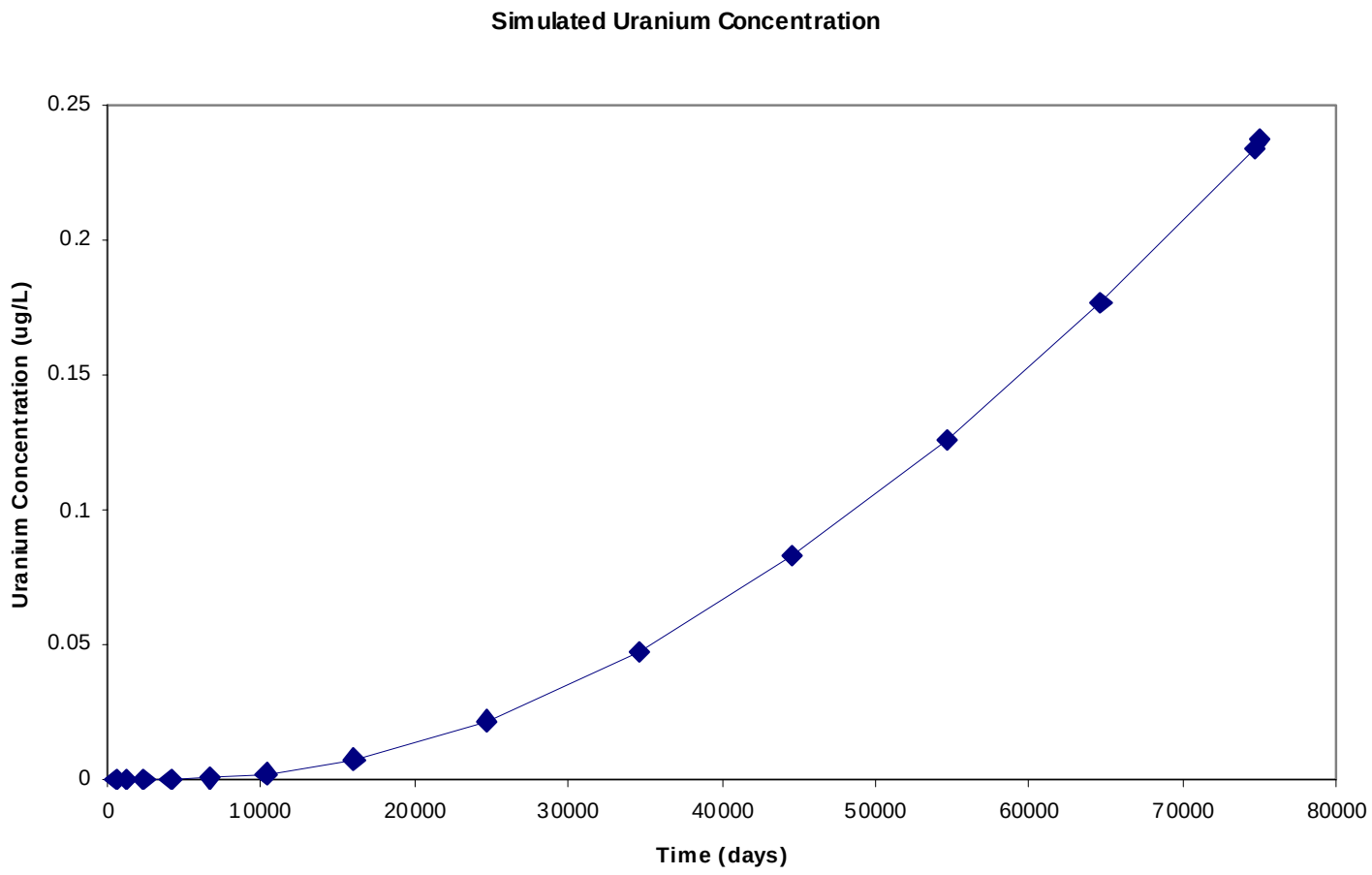


**Fig. 32. Uranium versus time at grid cell in Layer 4 (Jefferson City-Cotter HSU) near Deul's Mountain Source. (See "resident farmer" location in Fig. 31.)**

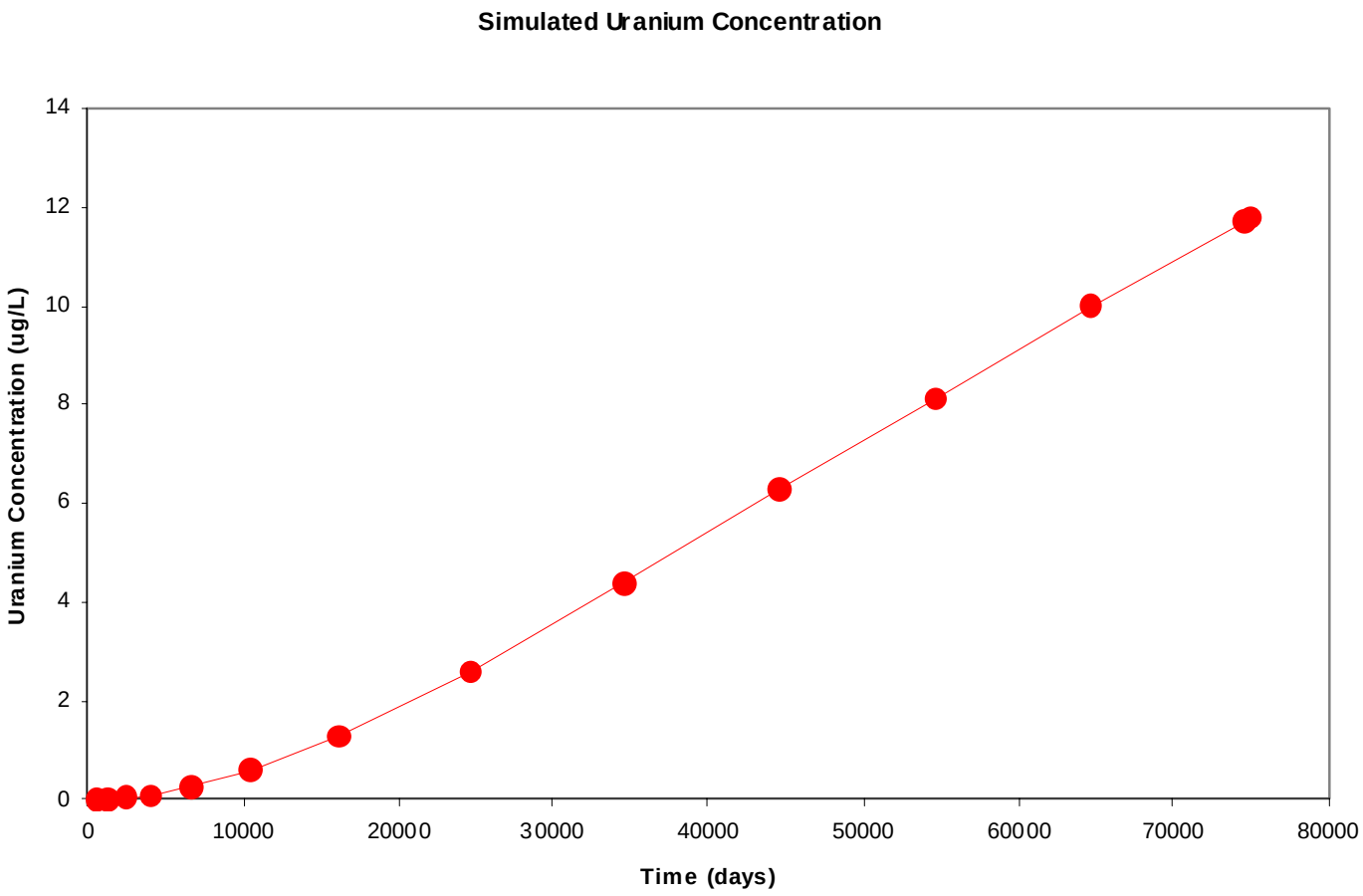


**Fig. 33. Uranium versus time at grid cell in Layer 4 (Jefferson City-Cotter HSU) near Burial Pits source. (See "resident farmer" location in Fig. 31.)**

**THIS PAGE INTENTIONALLY LEFT BLANK.**

# TABLES

**THIS PAGE INTENTIONALLY LEFT BLANK.**

**Table 1. Correspondence between hydrostratigraphic units and layers in the MODFLOW Model, including hydraulic conductivities assigned to layers and zones**

| HSU | Layer | Zone | Horizontal hydraulic conductivity ($K_h$) (ft/day) | Vertical anisotropy ($K_h/K_v$) |
|---|---|---|---|---|
| Shallow overburden | 1 | 1 | 0.3 | 1 |
| | | 2 | 0.3 | 1 |
| | | 3 | 50 | 1 |
| | | 4 | 0.3 | 1 |
| Deep overburden | 2 | 1 | 0.5 | 1 |
| | | 2 | 3 | 1 |
| | | 3 | 93 | 1 |
| | | 4 | 0.5 | 1 |
| Jefferson-City Cotter | 3 | - | 0.5 | 1 |
| | 4 | - | 5 | 5 |
| | 5 | - | 5 | 5 |
| Jefferson-City Cotter/Roubidoux Contact Zone | 6 | | 0.002 | 1 |
| | 7 | | 0.002 | 1 |
| | 8 | | 0.002 | 1 |
| Roubidoux | 9 | | 20 | 5 |

**THIS PAGE INTENTIONALLY LEFT BLANK.**